

*IN-02*  
*3-11-59*

# NASA

## MEMORANDUM

SUPERSONIC AND MOMENT-OF-AREA RULES COMBINED FOR RAPID  
ZERO-LIFT WAVE-DRAG CALCULATIONS

By Lionel L. Levy, Jr.

Ames Research Center  
Moffett Field, Calif.

**NATIONAL AERONAUTICS AND  
SPACE ADMINISTRATION**

WASHINGTON

June 1959



TABLE OF CONTENTS

SUMMARY . . . . .	1
INTRODUCTION . . . . .	2
LIST OF IMPORTANT SYMBOLS . . . . .	3
Subscripts . . . . .	4
Superscripts . . . . .	5
METHOD . . . . .	5
Basic Methods . . . . .	5
Supersonic area rule . . . . .	5
Moment-of-area rule . . . . .	7
Development of the Method . . . . .	9
Convergence problem . . . . .	10
Dimensionless drag equations . . . . .	11
Basic data, moments and lengths . . . . .	11
Procedure for Applying the Method . . . . .	13
General configurations . . . . .	13
Complete wings . . . . .	14
Airplane-type configurations . . . . .	16
Systems of bodies of revolution . . . . .	17
EVALUATION OF THE METHOD . . . . .	17
Accuracy . . . . .	18
Single body of revolution . . . . .	18
Pair of bodies of revolution . . . . .	18
Complete wings . . . . .	19
Airplane-type configurations . . . . .	20
Convergence problem . . . . .	20
Computing Time Required . . . . .	21
CONCLUDING REMARKS . . . . .	23
APPENDIX A - DIMENSIONLESS ZERO-LIFT WAVE-DRAG EQUATIONS . . . . .	25
APPENDIX B - CONCEPT OF SHEARED CONFIGURATIONS . . . . .	30
APPENDIX C - MOMENTS AND LENGTHS FOR SHEARED WINGS AND TAILS . . . . .	33
APPENDIX D - SAMPLE CALCULATIONS . . . . .	43
APPENDIX E - EVALUATION OF THE INTEGRAL FUNCTIONS FOR AIRFOIL SECTIONS WITH NONANALYTIC THICKNESS DISTRIBUTIONS . . . . .	50
REFERENCES . . . . .	53
FIGURES . . . . .	55



NATIONAL AERONAUTICS AND SPACE ADMINISTRATION

---

MEMORANDUM 4-19-59A

---

SUPERSONIC AND MOMENT-OF-AREA RULES COMBINED FOR RAPID

ZERO-LIFT WAVE-DRAG CALCULATIONS

By Lionel L. Levy, Jr.

SUMMARY

The concepts of the supersonic area rule and the moment-of-area rule are combined to develop a new method for calculating zero-lift wave drag which is amenable to the use of ordinary desk calculators. The total zero-lift wave drag of a configuration is calculated by the new method as the sum of the wave drag of each component alone plus the interference between components. In calculating the separate contributions each component or pair of components is analyzed over the smallest allowable length in order to improve the convergence of the series expression for the wave drag. The accuracy of the present method is evaluated by comparing the total zero-lift wave-drag solutions for several simplified configurations obtained by the present method with solutions given by slender-body and linearized theory. The accuracy and computational time required by the present method are also evaluated relative to the supersonic area rule and the moment-of-area rule.

The results of the evaluation indicate that total zero-lift wave-drag solutions for simplified configurations can be obtained by the present method which differ from solutions given by slender-body and linearized theory by less than 6 percent. This accuracy for simplified configurations was obtained from only nine terms of the series expression for the wave drag as a result of calculating the total zero-lift wave drag by parts. For the same number of terms these results represent an accuracy greater than that for solutions obtained by either of the two methods upon which the present method is based, except in a few isolated cases. For the excepted cases, solutions by the present method and the supersonic area rule are identical. Solutions by the present method are obtained in one fifth the computing time required by the supersonic area rule. This difference in computing time of course would be substantially reduced if the complete procedures for both methods were programed on electronic computing machines.

## INTRODUCTION

The supersonic area rule presented in reference 1 provides a useful tool for calculating the zero-lift wave drag at supersonic Mach numbers of configurations consisting of slender bodies, thin wings, and thin tails. The zero-lift wave drag of a given configuration was shown to be the average of the wave drag of a series of equivalent bodies of revolution. Since the development of the supersonic area rule, various numerical methods, easily adaptable to punch-card computing machines, have been developed for calculating the zero-lift wave drag of these equivalent bodies of revolution. To mention a few, references 2, 3, and 4, respectively, present methods based on a knowledge of the area distribution, the first derivative of the area distribution, and the second derivative of the area distribution of the equivalent bodies of revolution.

In reference 5 a method was developed for calculating zero-lift wave drag at low supersonic Mach numbers which does not require a knowledge of the equivalent bodies of revolution, but uses, instead, a convenient set of geometric parameters which are solely a function of the area and moment distributions of the given configuration. The geometric parameters consist of double moments of the area distribution of the given configuration calculated about both the streamwise and spanwise axes of the configuration. For this reason the method of reference 5 is referred to as the moment-of-area rule. With this method, it is practical to make zero-lift wave-drag calculations with ordinary desk calculators.

Similar to the supersonic area rule, the moment-of-area rule also evaluates a series expression for the zero-lift wave drag. As a result of a simplifying assumption the moment-of-area-rule series expression for the wave drag does not converge as rapidly as does that for the supersonic area rule. The accuracy and the number of double moments (terms of the series) required by the moment-of-area rule to obtain adequate convergence of the series at supersonic Mach numbers are too great for the method to be practical with desk calculators. At a Mach number of 1, however, the number of moments (calculated about only the spanwise axis of the given configuration) required are greatly reduced to the point where desk calculators are practical. It was reasoned, therefore, that if a convenient and systematic technique could be developed for calculating the moments of equivalent bodies of revolution, the concepts of the moment-of-area rule at Mach number 1 and the supersonic area rule could be combined to develop a method for calculating zero-lift wave drag for a wide range of Mach numbers by means of ordinary desk calculators. It is the purpose of this report to present the development and evaluation of such a method. The method will be evaluated by comparing results computed by the method developed herein with those obtained by other existing methods of calculation.

## LIST OF IMPORTANT SYMBOLS

$A_n(\beta, \theta)$	coefficients of a Fourier sine series expansion of $S'(x, \beta, \theta)$
$b$	wing span
$B$	$1 - \lambda$
$c$	wing chord at the vertical plane of symmetry
$d$	lateral distance between the longitudinal axes of a pair of bodies of revolution
$D(\beta)$	zero-lift wave drag of a configuration
$D(\beta, \theta)$	zero-lift wave drag of an equivalent body of revolution of a configuration
$K$	tangent of the sweep angle of the 50-percent chord line of any sheared panel of a wing or tail surface in dimensionless coordinates
$l$	length of a body of revolution
$l(\beta, \theta)$	length of an equivalent body of revolution
$M$	free-stream Mach number
$M_{pk}$	moments of the area distribution of a given configuration (see eq. (9))
$M_{Ok}(\beta, \theta)$	moments of the area distribution of an equivalent body of revolution
$N$	number of terms or harmonics used in the calculation of wave drag
$q$	free-stream dynamic pressure
$S(x, \beta, \theta)$	frontal projection of the area distribution intercepted on a given configuration by a set of parallel oblique planes tangent to the Mach cones
$t_0$	wing maximum thickness at the vertical plane of symmetry
$t(x, y)$	thickness distribution of a configuration

$x, y, z$	Cartesian coordinates in the free-stream, spanwise, and thickness directions, respectively
$\alpha$	local dimensionless airfoil-section chord station measured from the local 50-percent chord
$\beta$	$\sqrt{M^2 - 1}$
$\delta$	longitudinal distance between the lateral axes of a pair of sheared bodies of revolution
$\theta$	angle defining the orientation of the parallel oblique planes tangent to the Mach cones (see sketch (a))
$\lambda$	plan-form taper ratio
$\xi, \eta, \zeta$	dimensionless Cartesian coordinates in the free-stream, spanwise, and thickness directions, respectively
$\tau$	maximum thickness ratio
$\tau(\alpha)$	dimensionless thickness distribution of the local airfoil section
$\tau(\xi, \eta, K)$	dimensionless thickness distribution of one panel of a sheared plan form
$\Phi(\eta)$	spanwise variation of the dimensionless airfoil-section thickness along lines of constant percent chord

## Subscripts

$\left. \begin{array}{l} k, m, n, \\ p, r, s \end{array} \right\}$	indices of summation
I	interference conditions
L	lower panel of a plan form, $\eta < 0$
T	total
U	upper panel of a plan form, $\eta > 0$
W	wing panel alone conditions

- 1 properties of an exposed wing measured at or relative to the average chord at the wing-body juncture
- E,H component (body) E or component (body) H
- EH,UL interference, specifically, between bodies E and H or upper and lower wing panels, respectively

#### Superscripts

- ' differentiation with respect to a coordinate in the free-stream direction, except as noted in equation (C2)
- ~ dimensionless symbol

### METHOD

#### Basic Methods

Before the present method for calculating zero-lift wave drag is developed, it is well to review briefly the basic concepts of the two methods upon which the present analysis is based.

Supersonic area rule.- In reference 1 the zero-lift wave drag of configurations consisting of slender bodies, thin wings, and thin tail surfaces was shown to be the average of the wave drag of a series of equivalent bodies of revolution. This fact is given analytically by

$$D(\beta) = \frac{q}{8} \int_0^{2\pi} \sum_{n=1}^{\infty} n[A_n(\beta, \theta)]^2 d\theta \quad (1)$$

which, for convenience, is written

$$D(\beta) = \frac{1}{2\pi} \int_0^{2\pi} D(\beta, \theta) d\theta \quad (2)$$

where

$$D(\beta, \theta) = \frac{\pi}{4} q \sum_{n=1}^{\infty} n[A_n(\beta, \theta)]^2 \quad (3)$$

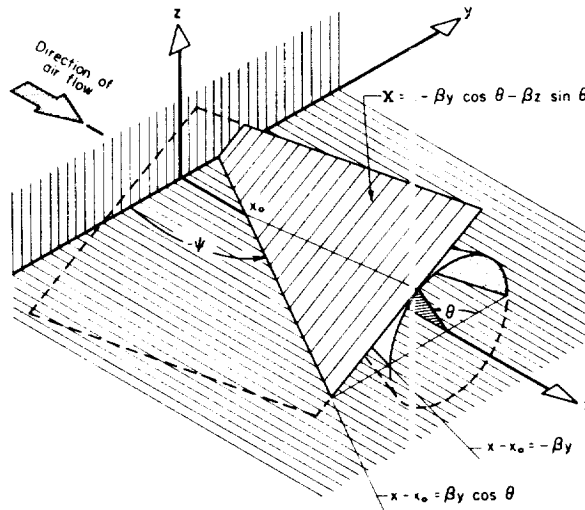
As defined in reference 1 the term  $D(\beta, \theta)$  is the zero-lift wave drag, as the Mach number approaches 1, of each equivalent body of revolution. For a given free-stream Mach number, or  $\beta$ , each value of  $\theta$  specifies one member of the series of equivalent bodies of revolution. The functions  $A_n(\beta, \theta)$  are coefficients of a Fourier sine series expansion of the first derivative of the area distribution of the equivalent bodies of revolution and are defined by

$$A_n(\beta, \theta) = \frac{2}{\pi} \int_{-\pi}^0 \frac{\partial S(x, \beta, \theta)}{\partial x} \sin(n\phi) d\phi \quad (4)$$

where

$$x = \frac{\lambda(\beta, \theta)}{2} \cos \phi \quad (5)$$

The normal cross-sectional area distribution of the equivalent bodies of revolution,  $S(x, \beta, \theta)$ , is obtained as the frontal projection of the area distribution intercepted on the given configuration by a set of parallel oblique planes tangent to the Mach cones. The term  $\lambda(\beta, \theta)$  is the length of the equivalent bodies of revolution. The coordinate system, angles, and Mach planes are defined in sketch (a).



Sketch (a)

Application of the basic methods is restricted to a particular group of configurations. This group satisfies the following conditions:

i. Body components and wing and tail components of a configuration are, respectively, sufficiently slender and sufficiently thin that only negligible errors are introduced into the calculation of  $S(x,\beta,\theta)$  by assuming the oblique planes to be normal to the horizontal plane.

ii. The area and first derivative of the area distribution of each equivalent body of revolution must not have discontinuities.

iii. The slope of the area distribution at the ends of each equivalent body of revolution must be zero.

The accuracy of the results obtained by the supersonic area rule depends upon the accuracy with which the Fourier coefficients are evaluated and upon the convergence of the series expression for the wave drag of each equivalent body given by equation (3). This latter dependency results from the fact that in practice the infinite series must be terminated at some finite number of terms. In references 2 and 3 the Fourier coefficients are evaluated from a knowledge of the area distribution and the first derivative of the area distribution of the equivalent bodies of revolution, respectively. In both references  $N = 25$  provides adequate convergence of the series for configurations which satisfy the restrictive conditions listed above. In reference 4 it was pointed out that for configurations which satisfied the above restrictive conditions but also had singularities at the ends of the second derivative of the area distribution of at least one component of the equivalent bodies of revolution, a larger number of terms was required to provide adequate convergence of the series. In this case all of the 49 available terms were required. Finally, equation (3) must be evaluated for enough values of  $\theta$  to define  $D(\beta,\theta)$  for integration.

Moment-of-area rule.- Zero-lift wave-drag calculations by the moment-of-area rule differ basically from those by the supersonic area rule in the manner in which the Fourier coefficients are evaluated. Unless all parts of a configuration lie within the nose Mach cone and the forward Mach cone from the tail, the equivalent body length,  $l(\beta,\theta)$ , will be greater than the actual length of the given configuration for some values of  $\theta$ . As shown in reference 5, however, by considering stream-wise body extensions of vanishingly small cross-sectional area, one can assume the length of each equivalent body of revolution to be constant and equal to or greater than the length of the longest equivalent body, say  $l$ . In this manner equation (5) becomes

$$x = l/2 \cos \varphi \quad (6)$$

As a result of this assumption the moment-of-area series expression for the zero-lift wave drag does not converge as rapidly as does that for the supersonic area rule. Upon substitution of equation (6) in equation (4) the Fourier coefficients can be expanded in a finite series expressible in

terms of a convenient set of geometric parameters,  $M_{pk}$ , and powers of  $\beta \cos \theta$  such that

$$A_n(\beta, \theta) = 2 \left(\frac{2}{l}\right)^2 \sum_{p=0}^{n-2} L_{np} (\beta \cos \theta)^p \quad (7)$$

where

$$L_{np} = \sum_{k=0}^{n-p-2} g_{npk} \left(\frac{2}{l}\right)^{p+k} M_{pk} \quad (8)$$

These geometric parameters are double moments of the thickness distribution of the given configuration calculated about both the streamwise ( $x$ ) and spanwise ( $y$ ) axes of the configuration. The origin of the coordinate system is located at the center of the configuration as indicated by the limits of integration in the following expression for the double moments (hereinafter referred to as moments):

$$M_{pk} = \frac{2}{\pi} \int_{-\frac{l}{2}}^{\frac{l}{2}} \int_{-\frac{b}{2}}^{\frac{b}{2}} t(x, y) x^k y^p dy dx \quad (9)$$

where  $t(x, y)$  is the thickness distribution of the given configuration and  $b/2$  is the wing semispan. In equation (8),  $g_{npk}$  are constant coefficients given by

$$g_{npk} = g_{nkp} = \left\{ \begin{array}{l} (-1)^{\frac{1}{2}(n-p-k-2)} \frac{(n-p-k-2) [(1/2)(n+p+k)]!}{[(1/2)(n-p-k-2)]!} \frac{2^k 2^p}{k! p!} \text{ for even values} \\ \text{zero otherwise} \end{array} \right\} \text{ of } (n-p-k) \quad (10)$$

Upon substitution of equation (7) in equation (3) and use of the result in equation (2), the integration with respect to  $\theta$  can be accomplished in closed form. In this manner the zero-lift wave drag at any supersonic Mach number is expressed in a series in powers of  $\beta$  with coefficients which are functions of the moments; that is,

$$D(\beta) = \frac{\pi}{4} q \sum_{n=2}^{\infty} n D_n(\beta) \quad (11)$$

where

$$D_n(\beta) = \frac{1}{2\pi} \int_0^{2\pi} [A_n(\beta, \theta)]^2 d\theta = 4 \left(\frac{2}{l}\right)^4 \left\{ \frac{1}{2\pi} \int_0^{2\pi} \left[ \sum_{p=0}^{n-2} L_{np}(\beta \cos \theta)^p \right]^2 d\theta \right\} \quad (12)$$

It is practical to determine the moments and make subsequent calculations of the zero-lift wave drag with ordinary desk calculators. Consequently, calculations by the moment-of-area rule are relatively simple compared to those by the supersonic area rule. However, as a result of using a constant length for each equivalent body of revolution, the moment-of-area-rule series expression for the wave drag does not converge as rapidly as does that for the supersonic area rule. Therefore, in order to obtain similar solutions by both methods more terms of the moment-of-area-rule drag equation must be employed. As pointed out in reference 5 for the moment-of-area rule and demonstrated in reference 4 for the supersonic area rule, the convergence of the series can be improved for each method by calculating the total zero-lift wave drag as the sum of the wave drag of each component alone plus the interference between components. For this procedure the smallest allowable length of each component or pair of components is employed in calculating the separate wave-drag contributions.

#### Development of the Method

The present method is developed by combining the concepts of the moment-of-area rule at Mach number 1 and the supersonic area rule. This combination consists merely of calculating the zero-lift wave drag by the moment-of-area rule at Mach number 1 for each equivalent body of revolution. For Mach number 1, equation (12) depends only upon the moments for  $p = 0$ , and can be written

$$D_n(M=1) = 4 \left(\frac{2}{l}\right)^4 L_{n0}^2 \quad (13)$$

where

$$L_{n0} = \sum_{k=0}^{n-2} \xi_{nok} \left(\frac{2}{l}\right)^k M_{0k} \quad (14)$$

Hence, for Mach number 1, equation (11) becomes

$$D(M=1) = \frac{\pi}{4} q \sum_{n=2}^{\infty} n D_n(M=1) \quad (15)$$

In view of equation (13), the zero-lift wave drag, at Mach number 1, of the equivalent bodies of revolution required by the supersonic area rule can be expressed as a function of the moments and lengths of the equivalent bodies as

$$D(\beta, \theta) = \frac{\pi}{4} q \left\{ 4 \left[ \frac{2}{l(\beta, \theta)} \right]^4 \sum_{n=2}^{\infty} n D_n(\beta, \theta) \right\} \quad (16)$$

where

$$D_n(\beta, \theta) = [L_{no}(\beta, \theta)]^2 \quad (17)$$

and

$$L_{no}(\beta, \theta) = \sum_{k=0}^{n-2} g_{nok} \left[ \frac{2}{l(\beta, \theta)} \right]^k M_{ok}(\beta, \theta) \quad (18)$$

In equation (18), the quantities  $M_{ok}(\beta, \theta)$  represent the moments of the equivalent bodies of revolution calculated about only the spanwise axis through the midpoint of the length of each equivalent body (see eq. (9) for  $p = 0$ ). From a comparison of equations (3) and (16) it is clear

that  $4 \left[ \frac{2}{l(\beta, \theta)} \right]^4 D_n(\beta, \theta)$  is merely the square of the Fourier coefficients.

Even though the concepts of the moment-of-area rule are employed to evaluate the Fourier coefficients, it should be noted that the actual length of each equivalent body,  $l(\beta, \theta)$ , is considered (see eqs. (16) and (18)). Finally the zero-lift wave drag of a given configuration is obtained by use of the results of equation (16) in equation (2).

Convergence problem.- Use of the moments to evaluate equation (17) permits zero-lift wave-drag calculations to be made with ordinary desk calculators. Experience has demonstrated, however, that the magnitude of the moments are such that six significant figures are required to obtain accurate results. As a consequence, it is not practical to make calculations for more than nine terms of the series ( $N = 9$ ) using desk calculators. In general, as few as nine terms will not provide adequate convergence of the series (see ref. 2). However, as suggested in reference 5 and demonstrated in reference 4, for any given number of terms the convergence of the series can be improved for multiple component

configurations by calculating the total zero-lift wave drag as the sum of that for each component alone plus the interference between components. As a result of the ease in finding  $M_{Ok}(\beta, \theta)$  for the various components of a given configuration compared to finding the area, the first derivative, or the second derivative of the area distribution of the components, the present method is more easily adapted to total zero-lift wave-drag calculations by this technique than are the methods of references 2, 3, and 4.

Dimensionless drag equations.- Zero-lift wave-drag calculations by the present method are most conveniently made using a dimensionless coordinate system. Consequently, the dimensionless quantities and zero-lift wave-drag equations for the present method are presented in appendix A. In appendix A the relationship between the dimensional and dimensionless zero-lift wave-drag equation for airplane-type configurations is shown to be

$$D(\beta) = \pi q \left( t_o \frac{b}{c} \right)^2 \left( \frac{b_1}{b} \right)^2 \left( \frac{\tau_1}{\tau} \right)^2 \tilde{D} \left( \beta \frac{b}{c} \right) \quad (19)$$

where

$$\tilde{D} \left( \beta \frac{b}{c} \right) = \frac{1}{2\pi} \int_0^{2\pi} \tilde{D} \left( \beta \frac{b}{c}, \theta \right) d\theta \quad (20)$$

$$\tilde{D} \left( \beta \frac{b}{c}, \theta \right) = \left[ \frac{c}{\lambda(\beta b/c, \theta)} \right]^4 \sum_{n=2}^{\infty} n \tilde{D}_n \left( \beta \frac{b}{c}, \theta \right) \quad (21)$$

$$\tilde{D}_n \left( \beta \frac{b}{c}, \theta \right) = \left[ \tilde{L}_{no} \left( \beta \frac{b}{c}, \theta \right) \right]^2 \quad (22)$$

$$\tilde{L}_{no} \left( \beta \frac{b}{c}, \theta \right) = \sum_{k=0}^{n-2} g_{nok} \left[ \frac{c}{\lambda(\beta b/c, \theta)} \right]^k \tilde{M}_{ok} \left( \beta \frac{b}{c}, \theta \right) \quad (23)$$

The subscript 1 in equation (19) indicates properties of the exposed wing measured at or relative to the average chord at the wing-body juncture.

Basic data, moments and lengths.- Success of the present method obviously depends upon a convenient technique for finding the moments and corresponding lengths of the various components of the equivalent bodies of revolution of a given configuration. The area distributions of body-of-revolution components of a configuration are independent of

Mach plane orientation. Consequently, the moments of body-of-revolution components are identical for all equivalent bodies of revolution. Furthermore, within the slenderness requirements of the basic methods, the normal cross-sectional area distribution of body-of-revolution components,  $S(x)$ , and the actual length of the body,  $l$ , can be employed. Hence for bodies of revolution

$$M_{ok} = \frac{2}{\pi} \int_{-\frac{l}{2}}^{\frac{l}{2}} S(x)x^k dx \quad (24a)$$

or in dimensionless coordinates (see appendix A)

$$\tilde{M}_{ok} = \frac{2}{\pi} \int_{-1}^1 \tilde{S}(\xi)\xi^k d\xi \quad (24b)$$

The area distributions and lengths of wing and tail components, on the other hand, change with Mach plane orientation. The concept of "sheared" configurations, which is briefly reviewed in appendix B, can be employed to find the area distributions of these equivalent-body components. In reference 4, the contribution of wing and tail components to the area distribution of the equivalent bodies of revolution was determined as a function of the tangent of the sweep angle of the 50-percent chord line of each sheared half plan form. For a given Mach number and Mach plane orientation, this single parameter ( $K$ , in dimensionless coordinates) relates each sheared half plan form to the proper equivalent body by the expressions (see appendix B)

$$\left. \begin{aligned} K_U &= K_O - \beta \frac{b}{c} \cos \theta \\ K_L &= K_O + \beta \frac{b}{c} \cos \theta \end{aligned} \right\} \quad (25)$$

where  $K_O$  is the tangent of the sweep angle of the 50-percent chord line of the given dimensionless plan form;  $K_U$  and  $K_L$  represent the tangent of the sweep angles of the sheared dimensionless half plan forms in the positive and negative  $\eta$  directions, respectively. As indicated by the subscripts U and L, these half plan forms hereinafter will be referred to as the upper and lower sheared half plan forms, respectively. The single parameter  $K$  is also used in appendix C of this report to determine the moments and lengths of the sheared half plan forms. From equation (25) it can be seen that the quantities in equations (20) to (23) which are a function of  $\beta b/c$  and  $\theta$  are a function of  $(\beta b/c)\cos \theta$ .

Procedure for Applying the Method

General configurations.- The total zero-lift wave drag of any general configuration is calculated by the present method as the sum of the wave drag of each component alone plus the interference between all pairs of components, as was described in reference 4. For instance, for a configuration with two components, E and H, the total zero-lift wave drag can be written

$$\tilde{D}_T \left( \beta \frac{b}{c} \right) = \tilde{D}_E \left( \beta \frac{b}{c} \right) + \tilde{D}_H \left( \beta \frac{b}{c} \right) + \tilde{D}_{EH} \left( \beta \frac{b}{c} \right) \quad (26)$$

where the first two terms represent the zero-lift wave drag of each component alone and are evaluated by equations (20) to (23) using the subscripts E and H in each of the equations. The last term represents the mutual interference between the two components and is evaluated by equation (20) using the subscripts EH and the following equations:

$$\tilde{D}_{EH} \left( \beta \frac{b}{c}, \theta \right) = 2 \left[ \frac{c}{l_{EH}(\beta b/c, \theta)} \right]^4 \sum_{n=2}^{\infty} n \tilde{D}_{EHn} \left( \beta \frac{b}{c}, \theta \right) \quad (27)$$

$$\tilde{D}_{EHn} \left( \beta \frac{b}{c}, \theta \right) = \tilde{L}_{Eno} \left( \beta \frac{b}{c}, \theta \right) \tilde{L}_{Hno} \left( \beta \frac{b}{c}, \theta \right) \quad (28)$$

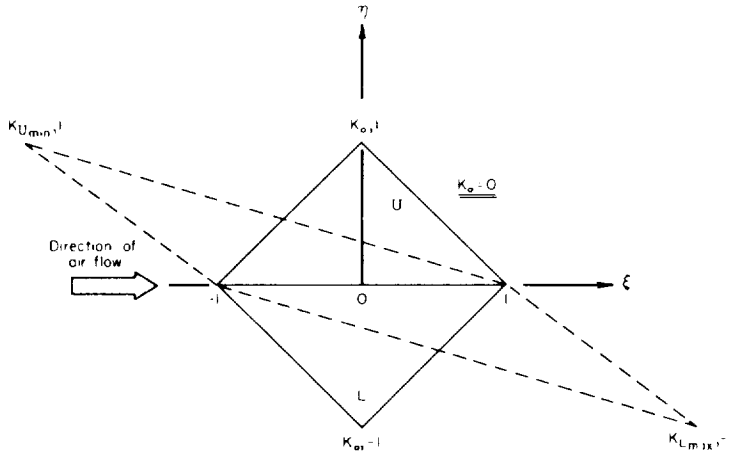
$$\tilde{L}_{Eno} \left( \beta \frac{b}{c}, \theta \right) = \sum_{k=0}^{n-2} g_{nok} \left[ \frac{c}{l_{EH}(\beta b/c, \theta)} \right]^k \tilde{M}_{Eok} \left( \beta \frac{b}{c}, \theta \right) \quad (29)$$

$$\tilde{L}_{Hno} \left( \beta \frac{b}{c}, \theta \right) = \sum_{k=0}^{n-2} g_{nok} \left[ \frac{c}{l_{EH}(\beta b/c, \theta)} \right]^k \tilde{M}_{Hok} \left( \beta \frac{b}{c}, \theta \right) \quad (30)$$

It is emphasized that all moments are calculated about the midpoint of the smallest allowable length of each component or pair of components for which the drag is to be computed. That is, in calculating the zero-lift wave drag of each component alone the smallest allowable length is obviously the separate length of each component. For the interference term, however,  $\tilde{M}_{Eok}(\beta b/c, \theta)$  and  $\tilde{M}_{Hok}(\beta b/c, \theta)$  are calculated about the midpoint of the total combined length of any two components.

Complete wings.- Assume that the total zero-lift wave drag is to be calculated at a specified supersonic Mach number,  $M_{max}$ , for a complete wing with  $0^\circ$  sweep of the 50-percent chord line ( $K_0 = 0$ ) as shown by the solid lines in sketch (b). With regard to the airfoil section it should

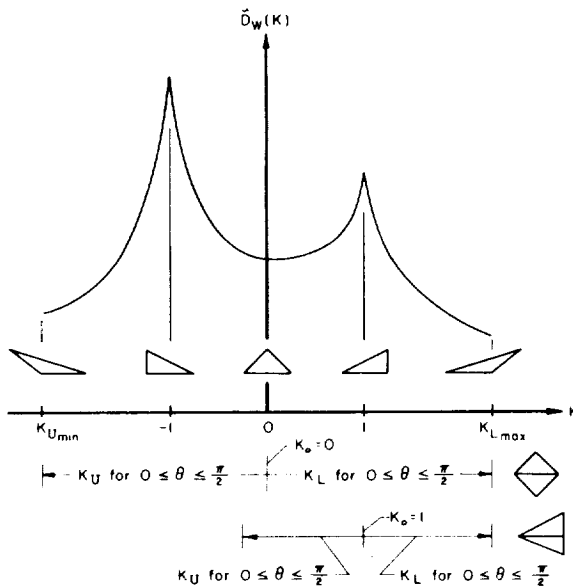
be recalled that at supersonic Mach numbers for which the Mach waves of the flow are inclined ahead of the wing leading edge the theory is applicable for arbitrary airfoil sections; that is, both round- and sharp-nosed sections. On the other hand, at higher supersonic Mach numbers for which the Mach waves of the flow are inclined behind the wing leading edge, the theory is applicable to wings with only a sharp-nosed airfoil section. For the problem assumed above consider a wing with sharp edges.



Sketch (b)

The calculations are initiated by a determination of the limiting values of  $K_{U_{min}}$  and  $K_{L_{max}}$  from equation (25) for  $\theta = 0$ . The corresponding sheared configuration is shown in sketch (b) by the dashed lines. (Note that  $|K_{U_{min}}|$  and  $|K_{L_{max}}|$  are greater than 1. If a round-nosed

airfoil section had been considered, these limiting values would be restricted to values less than 1.) The quantity  $\bar{D}_W(\beta b/c, \theta)$  or  $\bar{D}_W(K)$  is determined for one wing panel alone at arbitrary but sufficient values of  $K$  to define the curve shown in sketch (c). Addition of the two expressions in equation (25) relates the upper and lower wing panels in ordered pairs

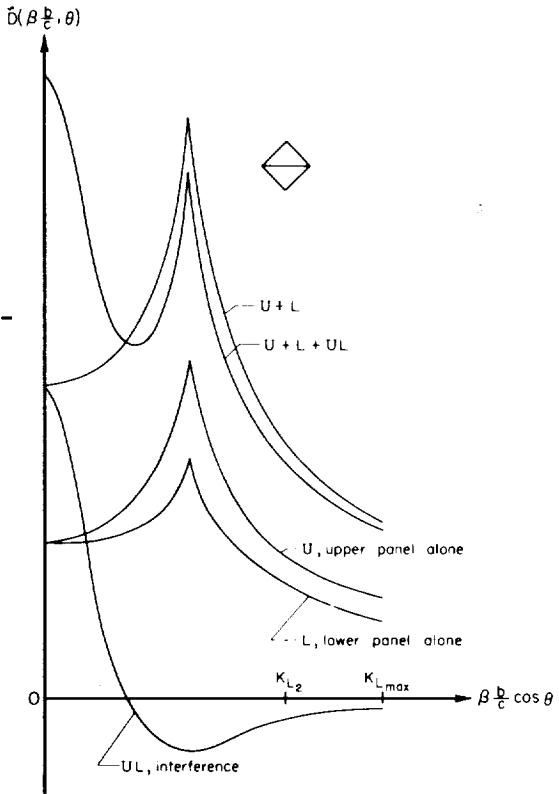


$$K_U + K_L = 2K_0 \quad (31)$$

By use of equation (31), the data in sketch (c) are used to make individual or combined plots of the zero-lift wave drag of each wing panel alone as a function

Sketch (c)

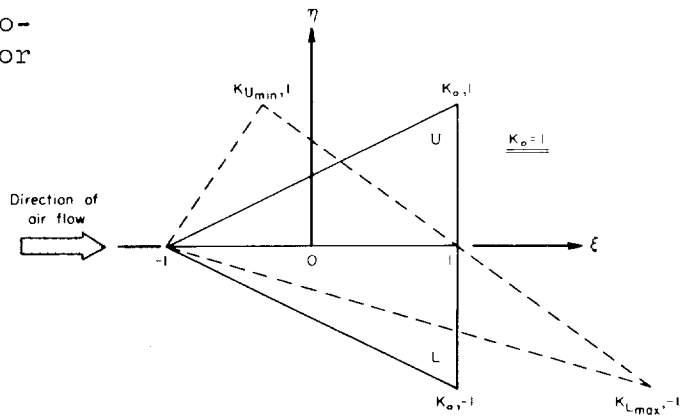
of  $(\beta b/c)\cos \theta$  (see sketch (d)). Since sheared configurations for complete wings are symmetrical in  $\pi/2$ , positive values of  $(\beta b/c)\cos \theta$  are more conveniently used for the abscissa for  $\pi/2 \geq \theta \geq 0$ ; hence, in sketch (d)  $0 \leq (\beta b/c)\cos \theta \leq K_{Lmax}$ . The interference between wing panels is calculated as a function of  $K_L$  but plotted directly as a function of  $(\beta b/c)\cos \theta$  as shown in sketch (d). The total zero-lift wave drag or the separate contributions can be obtained from the proper curve in sketch (d) by replotting the results against  $\theta$  for  $\pi/2 \geq \theta \geq 0$ . The resulting plot is then integrated graphically and this result is divided by  $\pi/2$  to obtain a dimensionless value of the zero-lift wave drag at  $M_{max}$  or  $(\beta b/c)_{max}$ . The drag in pounds is, of course, given by equation (19). It will be noted that for a complete wing  $(b_1/b)$  and  $(\tau_1/\tau)$  in equation (19) are unity.



Sketch (d)

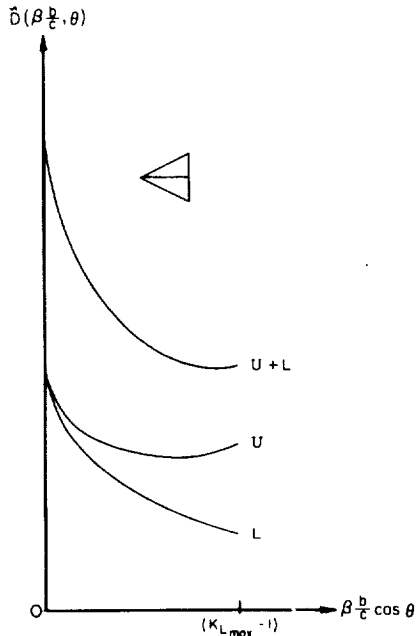
Once the zero-lift wave drag is calculated at  $M_{max}$  one has inherently obtained the data from which the drag can be calculated for all  $1 \leq M \leq M_{max}$ . For example, for  $1 < M_2 < M_{max}$  equation (25) yields a new maximum value of  $(\beta b/c)\cos \theta$  as  $K_{L2}$  (see sketch (d)). Hence, for  $(\beta b/c)_2 = K_{L2}$ , the portion of the curve in sketch (d) for  $0 \leq (\beta b/c)\cos \theta \leq K_{L2}$  can be replotted against  $\theta$  for  $\pi/2 \geq \theta \geq 0$ , graphically averaged, and divided by  $\pi/2$ . In this manner the zero-lift wave drag can be obtained for all  $1 \leq M \leq M_{max}$  or  $0 \leq (\beta b/c) \leq (\beta b/c)_{max}$ .

The basic data for one complete wing panel shown in sketch (c) can be used to calculate the drag of each wing panel of the complete wing shown in sketch (e). This wing differs from that of sketch (b) only by the sweep angle of the 50-percent chord line,  $K_0 = 1$ .



Sketch (e)

From use of  $K_0 = 1$  in equation (31) it is a simple matter to obtain  $\bar{D}(\beta b/c, \theta)$  from the data of sketch (c) in new ordered pairs for  $K_0 \leq K_L \leq K_{L_{max}}$ . With the aid of equation (25) these results for the wing panels alone are plotted for  $0 \leq (\beta b/c) \cos \theta \leq (K_{L_{max}} - 1)$  as shown



Sketch (f)

in sketch (f). Because the separate wing panels of the sheared configurations of the  $K_0 = 1$  plan form combine in different ordered pairs from those for the  $K_0 = 0$  plan form, the interference between wing panels will be different for each plan form. Consequently, additional calculations must be made for the interference between wing panels for the  $K_0 = 1$  plan form. It should be noted that the range of Mach numbers covered by the value  $(\beta b/c) \cos \theta = (K_{L_{max}} - K_0)$  will be different for each plan form.

Airplane-type configurations.— For a wing-body combination the zero-lift wave drag of the body alone is obtained from one set of calculations, since, as noted earlier,  $S(x, \beta, \theta)$  for each equivalent body of this component is assumed equal to  $S(x)$ . The wing-body interference is calculated as a function of  $K$  or  $(\beta b/c) \cos \theta$  and averaged graphically for selected values of  $\beta b/c$ . The exposed wing is treated in the same manner just described for a complete wing. In fact, in some instances,

the basic data,  $\tilde{D}_W(K)$ , for the wave drag of one panel of a complete wing can also be used to calculate the wave drag of each exposed wing panel alone of similar wings mounted on a body. This is possible whenever the dimensionless plan form of the exposed wing panel and of the complete wing panel are identical. As noted in appendix A, exposed wing panels are made dimensionless with respect to conditions at the wing-body juncture. Hence,  $\tilde{D}(K)$  for a complete wing panel can be used to calculate the wave drag of an exposed wing panel alone for all straight-line plan forms with zero taper ratio. For example, the wave drag of each of the exposed wing panels of the wings of sketches (b) and (e) mounted on a body can be computed as previously described using the data of sketch (c) for complete wings. The interference between exposed wing panels must be obtained by additional calculations since, for a given  $K$ , the combined length of both sheared wing panels is different for the exposed and complete dimensionless wings. In computing the drag in pounds the proper values of  $(b_1/b)$  and  $(\tau_1/\tau)$  must be inserted in equation (19).

Rather than present zero-lift wave drag as a function of Mach number, it has been found convenient to plot reduced drag as a function of  $\beta b/c$ . One can express equation (19) in coefficient form as

$$C_D = \frac{D}{qS} = \frac{\pi}{S} \left( t_0 \frac{b}{c} \right)^2 \left( \frac{b_1}{b} \right)^2 \left( \frac{\tau_1}{\tau} \right)^2 \tilde{D} \left( \beta \frac{b}{c} \right) \quad (32)$$

The wing aspect ratio  $A$  is given by  $b^2/S$  and the airfoil-section maximum thickness ratio,  $\tau$ , is given by  $t_0/c$ . Hence equation (32) can be written

$$\frac{C_D}{A\tau^2} = \pi \left( \frac{b_1}{b} \right)^2 \left( \frac{\tau_1}{\tau} \right)^2 \tilde{D} \left( \beta \frac{b}{c} \right) \quad (33)$$

Since  $b/c$  is proportional to aspect ratio, equation (33) is merely an expression of the linearized supersonic-flow similarity parameters; that is, the reduced wave-drag coefficient,  $C_D/A\tau^2$ , is a function of only  $\beta A$ . Thus, by making the calculations in dimensionless coordinates for a single configuration, one inherently computes the zero-lift wave drag for an entire family of related configurations.

Systems of bodies of revolution.- The principles of the foregoing analyses of airplane-type configurations can also be applied to systems of bodies of revolution. One first renders the system dimensionless as outlined in appendix A. The zero-lift wave drag can be calculated as noted earlier for each body alone. The interference between all pairs of bodies can be obtained in a manner similar to that described for complete wing panels merely by using the parameter  $\delta$  (see appendix B) rather than  $K$ . A technique for finding the equivalent-body length and the moments of any two sheared bodies about the midpoint of their combined length as a function of  $\delta$  can be obtained by following the same technique outlined in appendix C for the interference between wing panels. It should be noted, however, that the sheared configurations of a pair of bodies of revolution are symmetrical in  $\pi$  rather than  $\pi/2$  as in the case of wings and horizontal tails. If an electronic computing machine is available, more accurate results for systems of bodies of revolution can be obtained more rapidly by the method of reference 4 than by the present method.

#### EVALUATION OF THE METHOD

The accuracy and computational time required of the present method will be evaluated by comparing zero-lift wave-drag solutions for several simplified configurations computed by the present method with solutions obtained by other methods. Sample calculations for the solutions obtained by the present method are presented in appendix D.

## Accuracy

Single body of revolution.- Consider the very special case of a Sears-Haack body of revolution at  $M = 1$ . As shown by slender-body theory in reference 6, this body has minimum zero-lift wave drag at sonic speed for a given length and volume. The area distribution of this body is given by

$$S(x) = S_0 \left[ 1 - \left( \frac{2x}{l} \right)^2 \right]^{\frac{3}{2}} \quad (34)$$

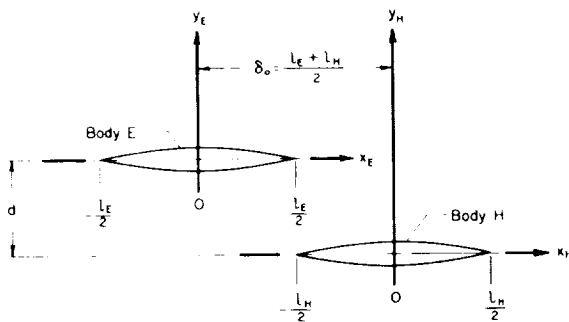
where  $S_0$  is the maximum frontal area of the body and  $l$  is the total body length.

As shown in appendix A of this report the zero-lift wave drag of a system of bodies of revolution can be expressed in terms of the dimensionless drag as

$$D = \pi q \left( \frac{S_0}{l/2} \right)^2 \tilde{D} \left( \beta \frac{d}{l} \right) \quad (35)$$

According to reference 6 the slender-body-theory value of  $\tilde{D}(\beta d/l)$  at  $M = 1$  is  $9/8$ . Zero-lift wave-drag calculations by the present method yield exactly  $9/8$  (see appendix D). It is interesting to note that the series expression for the zero-lift wave drag converges absolutely for the term  $n = 2$ . The contribution of all other terms is identically zero. This result further demonstrates that a Sears-Haack body has minimum zero-lift wave drag at  $M = 1$  for a given length and volume. That is,  $\tilde{M}_{00}$  is proportional to the volume of a configuration (see eq. (9) for  $p = 0$ ) and this moment alone appears only in the  $n = 2$  term (see appendix A).

Pair of bodies of revolution.- Dimensionless zero-lift wave-drag values have been calculated at  $M = 1$  for the pair of Sears-Haack bodies shown in sketch (g). Values computed by the present method (see appendix D) are tabulated below together with analytical values obtained by slender-body theory from reference 4. The total zero-lift wave drag calculated by the present method is accurate to within 5.3 percent of the slender-body-theory solution of reference 4. As noted earlier for a single body of revolution, values for the bodies



Sketch (g)

$\bar{D}[\beta(d/l)]$ for bodies in sketch (g), $M = 1$		
Drag component	Present method	Reference 4
Body E alone	1.125	1.125
Body H alone	1.125	1.125
Interference	.204	.340
Total	2.454	2.590

alone by the present method are in exact agreement with the analytical solutions of reference 4 but the interference values agree to within only 40 percent. This large discrepancy for the interference calculation results from the fact that the moments for this calculation must be calculated about the midpoint of the combined length of both bodies, a length longer than that of the individual bodies. As noted in reference 5, when this occurs the contributions to the drag of the terms for  $n > 9$  (higher harmonics) become significant.

Complete wings.- Zero-lift wave-drag calculations have been made for two families of complete wings with biconvex airfoil sections and a constant thickness ratio from root to tip. One family has a diamond plan form ( $K_0 = 0$ ) and the other a triangular plan form ( $K_0 = 1$ ) as shown in sketches (b) and (e), respectively. The linearized theory zero-lift wave-drag solutions for these wings have been obtained in reference 7 by a stepwise integration of the pressures over the entire wings. The zero-lift wave-drag results from reference 7 and those obtained from calculations by the present method for  $N = 9$  (see appendix D) are presented in figure 1 in reduced drag-coefficient form. In order to evaluate the present method relative to the method of the supersonic area rule and the moment-of-area rule, zero-lift wave-drag solutions for both families of complete wings were calculated by both latter methods, the two methods upon which the present method is based. These latter results are also presented in figure 1. Results for the supersonic area rule are usually obtained by the method of reference 2. In this report, however, the results for  $N = 9$  were obtained by the technique of the present method by calculating the total moments of each equivalent body about the midpoint of the total length of each sheared configuration. By this approach the equivalent-body zero-lift wave-drag equations for the present and supersonic-area-rule methods can be shown to be identical theoretically. Numerical calculations by both methods ( $N = 9$ ) for several equivalent bodies agreed to within one half of 1 percent. Results for the moment-of-area rule were calculated for  $N = 9$  by the alternative drag formula given in appendix C of reference 5. As indicated in figure 1, for the range of values of  $\beta b/c$  for which data are available, the present method yields results which differ from the linearized-theory solutions of reference 7 between 1 and 6 percent. The data of figure 1 also indicate that the solutions obtained by the present method are more accurate than those obtained by the other two methods. Furthermore,

solutions obtained by the supersonic area rule are more accurate than those obtained by the moment-of-area rule. The more accurate solutions by the present method are a result of calculating the drag of the wings by parts. Since the solutions obtained by the three "series" methods were calculated for  $N = 9$  in each case, the relative accuracy of the solutions obtained by these three methods is associated with the relative rapidity of the convergence of the series expression of the zero-lift wave drag for each method. The relative convergence of the series for the three methods will be discussed subsequently.

Airplane-type configurations.- The procedures for applying the present method to airplane-type configurations have been discussed earlier in this report and in appendix A. Although no calculations have been made to evaluate the accuracy of the present method for calculating the zero-lift wave drag of such configurations relative to other methods, it is felt that differences in such solutions would be comparable to those discussed above for complete wings. However, it should be noted that, as discussed in appendix A, some errors, not present in the case of complete wings, might be introduced into the calculations by the present method as a result of assuming a constant wing station for the wing-body juncture when computing the moments of the exposed wing panels. These errors will be more significant in cases of severely indented bodies and in cases where the body radius is of the same order of magnitude as the wing thickness at the wing-body juncture.

Convergence problem.- As mentioned in reference 5, in the Fourier series analysis of the slope of the area distribution of a configuration (a type of analysis basic to the present method, the supersonic area rule and the moment-of-area rule), the series converges most rapidly when the smallest allowable length of the configuration is used in the wave-drag analysis. The total zero-lift wave-drag results shown in figure 1 for the moment-of-area rule used a constant total length as specified in appendix C of reference 5. The supersonic area rule employed the total length of each individual sheared complete wing. Use of the individual total lengths with the supersonic area rule results in a marked increase in the rapidity with which the series converges. This is indicated in figure 1 by the larger values of the wave drag obtained by the supersonic area rule as compared to those obtained by the moment-of-area rule. The total zero-lift wave drag was calculated by the present method as the sum of the wave drag of each wing panel alone plus the interference between wing panels. The individual length of each wing panel of each sheared configuration was used for the drag calculations of each wing panel alone and the combined length of both sheared wings panels was used for the interference calculations. In this manner the present method provided an additional increase in the rate at which the series converges. Thus, the values of the wave drag in figure 1 for the present method are greater than those obtained by the supersonic area rule and the moment-of-area rule.

Regardless of whether the total zero-lift wave-drag calculations are made using the smallest allowable length or the total length of each sheared configuration, the interference calculations in both cases are made using the total length. On the other hand, calculations of the wave drag of each wing panel alone are made using either the length of each sheared wing panel or the combined length of both sheared wing panels. Hence, the magnitude of the increased accuracy of the total zero-lift wave-drag calculations afforded by the use of the smallest allowable length depends upon the ratio of the length of each sheared wing panel alone to the combined length of both sheared wing panels. For convenience this ratio is designated by  $\epsilon$ . The smaller the value of  $\epsilon$  compared to unity the greater will be the improvement in the drag calculations as a result of using the smallest allowable rather than the total length. This fact is demonstrated by the data in figure 1. Up to a Mach number for a sonic leading edge for the diamond plan form ( $\beta b/c = 1$  in fig. 1(a))  $\epsilon = 1$  for both wing panels of all sheared configurations; hence, the single curve for the results of the present and supersonic-area-rule methods in this region. For  $\beta b/c > 1$ ,  $\epsilon$  is less than 1 for only some of the sheared configurations and is also the same value for both wing panels. In this region, therefore, only a very slight improvement in the accuracy of the solutions obtained by the present method is realized compared to solutions obtained by the supersonic area rule. For the triangular plan form (fig. 1(b))  $\epsilon = 1$  only for  $\theta = \pi/2$  or for  $\beta b/c = 0$ . For all other sheared configurations  $\epsilon < 1$  and has different values for each wing panel. Thus, the accuracy of the solutions obtained by the present method for the triangular plan form is substantially improved compared to the accuracy of the solutions obtained by the supersonic area rule.

In view of the benefits demonstrated above resulting from the calculation of total zero-lift wave drag by parts, the question naturally arises as to the possibility of using this procedure in conjunction with the supersonic area rule. The method of reference 2 can, in fact, be adapted to such a procedure. This, however, is not recommended unless one is prepared to accept a two- to threefold increase in work load.

#### Computing Time Required

The method of reference 7 uses the pressures over the entire wing plan form to calculate total zero-lift wave drag. These calculations are necessarily tedious and lengthy. The actual computational time is not given in reference 7. However, from a comparative examination of the wave-drag equations this method obviously requires more computational time than the present method or the two methods upon which the present method is based. Furthermore, the latter three methods each employ

some geometric property of the configuration to evaluate the Fourier coefficients of a series expression for the wave drag. For these reasons the computational time required of present method is evaluated relative to only the supersonic area and moment-of-area rules. The computational time in each case is based on a series for  $N = 9$ .

The basic differences in the computational time required of the moment-of-area rule, the present method, and the supersonic area rule are a function of the time required by each method to obtain the respective geometric properties used to evaluate the Fourier coefficients. The actual time, of course, depends upon the complexity of each configuration. The total zero-lift wave-drag calculations for the diamond-plan-form wing by the moment-of-area rule required 20 man-hours with desk calculators. By this method the  $\tilde{M}_{pk}$  for only the original complete wing were required. No graphical averaging was required. The present method, applied with either the smallest allowable or the total length, required 100 man-hours with desk calculators. By this method the  $\tilde{M}_{Ok}(\beta b/c, \theta)$  for 20 sheared configurations were used. The wave-drag results for these configurations were graphically averaged. No calculations were actually made by the supersonic area rule; however, a computing time of 500 man-hours has been estimated for this method by the authors of reference 2. This large estimate was based primarily upon the determination, with desk calculators, of the area distribution of the 20 sheared configurations and secondarily upon a graphical averaging of the wave-drag results.

The basic data for the wave drag of each sheared wing panel alone of the diamond plan form was used in the manner described in the METHOD section to obtain the wave drag of each wing panel alone of the triangular plan form. The only additional calculation required to obtain the total zero-lift wave drag of the triangular plan form by the present method was that for the interference between wing panels and, of course, the graphical averaging of all results. In this manner only 30 man-hours were required by the present method to obtain the results for the triangular-plan-form wing as compared to 100 man-hours for the diamond-plan-form wing. Similar to the case of the diamond-plan-form wing the moment-of-area-rule calculations required 20 man-hours for the triangular plan form. Since the method of reference 2 does not normally yield the wave drag by parts, zero-lift wave-drag calculations by this method would also require an estimated 500 man-hours for the triangular-plan-form wing.

The 500 man-hour computation for the supersonic area rule was made without a knowledge of reference 4 or the present report which both utilize the parameter  $K$  to organize the basic data for wings. It is reasonable to expect, therefore, that use of the parameter  $K$ , and/or making calculations for related wing by parts, would result in a lower estimate of the computing time required of the supersonic area rule. Furthermore, the differences in computing time, of course, would be substantially reduced

if the complete procedures for all methods were programed on electronic computing machines. It is emphasized, however, that the time required to program each method would be different and is unknown at present.

#### CONCLUDING REMARKS

A method has been developed for calculating zero-lift wave drag by combining the concepts of the supersonic area rule and the moment-of-area rule. The accuracy of the method has been evaluated by comparing total zero-lift wave-drag solutions obtained for several simplified configurations by the present method with solutions given by slender-body and linearized theory. The accuracy and computing time required of the method have also been evaluated relative to the two methods upon which the present method is based. The following remarks are warranted as a result of the development and evaluation of the present method.

Results are obtained by the present method from a series expression for the zero-lift wave drag which can be evaluated with an ordinary desk calculator. The total zero-lift wave drag of a configuration is calculated as the sum of the wave drag of each component alone plus the interference between components. Total wave-drag results for several simplified configurations demonstrated that, by calculating the total drag by parts, nine terms provide adequate convergence of the series. Total zero-lift wave-drag results obtained by the present method differed from solutions given by slender-body and linearized theory by less than 6 percent for all configurations investigated. For nine terms of the wave-drag series, these results represent an accuracy greater than that obtained by the moment-of-area rule and greater than or equal to in some isolated cases, the results obtained by the supersonic area rule. The greater accuracy of the present method is a direct result of calculating the total zero-lift wave drag by parts.

The computational time required by the present method was five times as great as that required by the moment-of-area rule and one-fifth of that required of the supersonic area rule. The shorter computing time of the moment-of-area rule, however, is of no real consequence in view of the poor accuracy of results obtained by this method. The differences in computing time, of course, would be substantially reduced if the complete procedures for all methods were programed on electronic computing machines.

As a result of making the calculations in dimensionless coordinates the basic data obtained for a configuration at a specified supersonic Mach number can be manipulated to obtain the total zero-lift wave drag

of the given configuration for all lower supersonic Mach numbers with a minimum of additional calculations. Furthermore, the basic data for a given configuration which is used to calculate the wave drag of each wing panel alone can be manipulated to provide the wave drag of each wing panel alone of an entire family of similar wings which differ only in sweep.

Ames Research Center

National Aeronautics and Space Administration

Moffett Field, Calif., Jan. 19, 1959

## APPENDIX A

## DIMENSIONLESS ZERO-LIFT WAVE-DRAG EQUATIONS

In order to take advantage of the decrease in the number of parameters resulting from similarity considerations, and to facilitate the calculations, the quantities defined in the METHOD section can be made dimensionless.

## AIRPLANE-TYPE CONFIGURATIONS

## Complete Wings Alone

As shown in appendix B of reference 5, all  $x$  coordinates can be divided by the half-chord of the wing at the vertical plane of symmetry,  $c/2$ ; all  $y$  coordinates can be divided by the semispan of the complete wing,  $b/2$ ; and all  $z$  or thickness coordinates,  $t$ , can be divided by the wing maximum thickness at the vertical plane of symmetry,  $t_0$ . In this manner the dimensionless quantities and their relationship to the corresponding dimensional quantities can be defined as follows: The dimensionless Cartesian coordinates are defined by

$$\left. \begin{aligned} \xi &= \frac{2x}{c} \\ \eta &= \frac{2y}{b} \\ \zeta &= \frac{z}{t_0} \quad \text{or} \quad \tau(\xi, \eta) = \frac{t(x, y)}{t_0} = \frac{t(\xi, \eta)}{t_0} \end{aligned} \right\} \quad (A1)$$

The moments for the equivalent bodies of revolution can be written with the aid of equation (9), for  $p = 0$ , as

$$M_{ok}(\beta, \theta) = \frac{2}{\pi} \int_{-\frac{b}{2}}^{\frac{b}{2}} \int_{-\frac{l(\beta, \theta)}{2}}^{\frac{l(\beta, \theta)}{2}} t(x, y, \beta, \theta) x^k dx dy \quad (A2)$$

With the definitions of equation (A1), equation (A2) is made dimensionless as follows:

$$\tilde{M}_{ok} \left( \beta \frac{b}{c}, \theta \right) = \frac{M_{ok}(\beta, \theta)}{t_o \left( \frac{b}{2} \right) \left( \frac{c}{2} \right)^{k+1}} = \frac{2}{\pi} \int_{-1}^1 \int_{-\frac{l(\beta b/c, \theta)}{c}}^{\frac{l(\beta b/c, \theta)}{c}} \tau \left( \xi, \eta, \beta \frac{b}{c}, \theta \right) \xi^k d\xi d\eta \quad (A3)$$

For the  $L_{no}(\beta, \theta)$  of equation (18)

$$\tilde{L}_{no} \left( \beta \frac{b}{c}, \theta \right) = \frac{L_{no}(\beta, \theta)}{t_o \left( \frac{b}{2} \right) \left( \frac{c}{2} \right)} = \sum_{k=0}^{n-2} \mathfrak{E}_{nok} \left[ \frac{c}{l(\beta b/c, \theta)} \right]^k \tilde{M}_{ok} \left( \beta \frac{b}{c}, \theta \right) \quad (A4)$$

Hence,

$$\tilde{D}_n \left( \beta \frac{b}{c}, \theta \right) = \frac{D_n(\beta, \theta)}{\left[ t_o \left( \frac{b}{2} \right) \left( \frac{c}{2} \right) \right]^2} = \left[ \tilde{L}_{no} \left( \beta \frac{b}{c}, \theta \right) \right]^2 \quad (A5)$$

Finally, the relationship between the dimensional and dimensionless zero-lift wave drag for an equivalent body of revolution of a complete wing is given by (see eq. (16))

$$D(\beta, \theta) = \pi q \left( t_o \frac{b}{c} \right)^2 \tilde{D} \left( \beta \frac{b}{c}, \theta \right) \quad (A6)$$

where

$$\tilde{D} \left( \beta \frac{b}{c}, \theta \right) = \left[ \frac{c}{l(\beta b/c, \theta)} \right]^4 \sum_{n=2}^{10} n \tilde{D}_n \left( \beta \frac{b}{c}, \theta \right) \quad (A7)$$

Inspection of equation (2) indicates that for a given configuration

$$D(\beta) = \pi q \left( t_o \frac{b}{c} \right)^2 \tilde{D} \left( \beta \frac{b}{c} \right) \quad (A8)$$

where

$$\tilde{D} \left( \beta \frac{b}{c} \right) = \frac{1}{2\pi} \int_0^{2\pi} \tilde{D} \left( \beta \frac{b}{c}, \theta \right) d\theta \quad (A9)$$

### Wings in the Presence of Bodies

For a given configuration the present method requires separate calculations of the wave drag of each component alone. Hence, the  $\eta$  limits of integration in equation (A3) for one panel of an exposed wing (or tail) would be from the wing-body juncture,  $\eta = \eta_1(\xi)$ , to the wing tip,  $\eta = 1$ . Calculation of the moments is obviously simplified if the  $\eta$  limits of integration are constant from 0 to 1. This is accomplished by assuming a constant wing station for the wing-body juncture which is an average wing station of the actual juncture and by rendering the resulting exposed wing panel dimensionless with respect to the conditions at this averaged wing-body juncture. Use of the averaged wing-body juncture rather than the contour of the actual wing-body juncture has been found to have a negligible effect upon the drag calculations except in cases of severe body indentations and in cases where the body radius is of the same order of magnitude as the wing thickness at the wing-body juncture. Thus, the  $x$  coordinates can be divided by the half-chord of the wing at the juncture,  $c_1/2$ , the  $y$  coordinates can be divided by the semispan of the exposed wing,  $b_1/2$ , and the thickness coordinates can be divided by the wing maximum thickness at the juncture,  $t_1$ . In this manner equation (A8) can be written

$$D(\beta) = \pi q \left( t_1 \frac{b_1}{c_1} \right)^2 \tilde{D} \left( \beta \frac{b_1}{c_1} \right) \quad (A10)$$

Most practical wing (or tail) plan forms have straight leading and trailing edges; hence,  $b_1/c_1 = b/c$ . It is convenient, therefore, to write equation (A10) in a form similar to that of equation (A8); that is,

$$D(\beta) = \pi q \left( t_0 \frac{b}{c} \right)^2 \left( \frac{b_1}{b} \right)^2 \left( \frac{\tau_1}{\tau} \right)^2 \tilde{D} \left( \beta \frac{b}{c} \right) \quad (A11)$$

where

$$\left. \begin{aligned} \tau &= \frac{t_0}{c} \\ \tau_1 &= \frac{t_1}{c_1} \end{aligned} \right\} \quad (A12)$$

## SYSTEMS OF BODIES OF REVOLUTION

## Single Body of Revolution

The moments of a single body of revolution are determined from the area distribution of the body as given by equation (24a); that is,

$$M_{ok} = \frac{2}{\pi} \int_{-\frac{l}{2}}^{\frac{l}{2}} S(x) x^k dx \quad (A13)$$

It is convenient, therefore, to render a body of revolution dimensionless by dividing the  $x$  coordinates by the half-body length,  $l/2$ , and by dividing the area distribution by the maximum frontal area of the body,  $S_0$ . Thus

$$\left. \begin{aligned} \xi &= \frac{2x}{l} \\ \tilde{S}(\xi) &= \frac{S(x)}{S_0} = \frac{S(\xi)}{S_0} \end{aligned} \right\} \quad (A14)$$

In this manner the dimensionless moments of equation (A13) can be defined as

$$\tilde{M}_{ok} = \frac{M_{ok}}{S_0 (l/2)^{k+1}} = \frac{2}{\pi} \int_{-1}^1 \tilde{S}(\xi) \xi^k d\xi \quad (A15)$$

Equations for  $\tilde{L}_{n0}$ ,  $\tilde{D}_n$ , and  $\tilde{D}$  for a single body of revolution are obtained from equations (A4), (A5), and (A7), respectively, by replacing  $t_0(b/l)$  and  $c/2$  by  $S_0$  and  $l/2$ , respectively. A single body, of course, is independent of  $\beta$  and  $\theta$ . Hence, from equation (A6) or (A8) the relationship between the dimensional and dimensionless zero-lift wave drag for a single body of revolution is given by

$$D = \pi q \left( \frac{S_0}{l/2} \right)^2 \tilde{D} \quad (A16)$$

## Two or More Bodies of Revolution

Individual dimensionless coordinate systems are used to calculate the wave drag of each body alone. To calculate the interference between pairs of bodies of revolution, however, it has been found more convenient to render each pair of bodies dimensionless with respect to the length and maximum frontal area of only one of the bodies. Usually the largest body is selected. The dimensionless quantities  $\tilde{L}_{n0}$ ,  $\tilde{D}_n$ , and  $\tilde{D}$  for interference calculations between pairs of sheared bodies (see appendix B) are obtained in the manner described above for a single body. In addition, quantities which are a function of  $(\beta b/c, \theta)$  are replaced by  $(\beta d/l, \theta)$ , where  $d$  is the lateral spacing of the bodies, as shown for example in sketch (g), and  $l$  is the length of that body upon which the dimensionless quantities are based.

For the convenience of those who may use the present method the  $\tilde{L}_{n0}(\beta b/c, \theta)$  of equation (A4) are listed below for  $n$  up to and including 9. The parameters  $\beta b/c$  and  $\theta$  have been omitted from the notation in the interest of simplicity.

$$\begin{aligned}
 \tilde{L}_{20} &= \tilde{M}_{00} \\
 \tilde{L}_{30} &= 4(c/l)\tilde{M}_{01} \\
 \tilde{L}_{40} &= -2\tilde{M}_{00} + 12(c/l)^2\tilde{M}_{02} \\
 \tilde{L}_{50} &= -12(c/l)\tilde{M}_{01} + 32(c/l)^3\tilde{M}_{03} \\
 \tilde{L}_{60} &= 3\tilde{M}_{00} - 48(c/l)^2\tilde{M}_{02} + 80(c/l)^4\tilde{M}_{04} \\
 \tilde{L}_{70} &= 24(c/l)\tilde{M}_{01} - 160(c/l)^3\tilde{M}_{03} + 192(c/l)^5\tilde{M}_{05} \\
 \tilde{L}_{80} &= -4\tilde{M}_{00} + 120(c/l)^2\tilde{M}_{02} - 480(c/l)^4\tilde{M}_{04} + 448(c/l)^6\tilde{M}_{06} \\
 \tilde{L}_{90} &= -40(c/l)\tilde{M}_{01} + 480(c/l)^3\tilde{M}_{03} - 1344(c/l)^5\tilde{M}_{05} + 1024(c/l)^7\tilde{M}_{07}
 \end{aligned}
 \tag{A17}$$

## APPENDIX B

## CONCEPT OF SHEARED CONFIGURATIONS

With the supersonic area rule, one calculates the zero-lift wave drag of a configuration as the average of that of a series of equivalent bodies of revolution. The normal cross-sectional area distribution of these equivalent bodies is obtained as the frontal projection of the area distribution intercepted on the given configuration by a set of parallel oblique planes tangent to the Mach cones. In reference 8 a new concept was first introduced which permits the use of the normal cross-sectional area distributions of a series of sheared configurations which, within the slenderness requirements of the supersonic area rule, are considered equal to those of the equivalent bodies obtained in the manner just described. In reference 4 the concept of sheared configurations was employed as a simplified technique for finding the contribution of wings, tails, and pairs of bodies of revolution to the area distribution of the equivalent bodies of revolution. The present method employs the concept of sheared configurations as a simplified technique for finding the moments and lengths of the various components of the equivalent bodies of revolution. Therefore, a brief review of this concept is presented below for wings, tails, and pairs of bodies of revolution.

## WINGS AND TAILS

## Wings

Complete wings.- A complete wing is shown in dimensionless coordinates by the solid lines in figure 2(a). This wing is made dimensionless with respect to conditions at the vertical plane of symmetry (see appendix A). The traces in the  $\xi, \eta$  plane (see fig. 2(a)) made by the intersection of the oblique planes and the  $\xi, \eta$  plane are inclined to the  $\eta$  axis at an angle  $\tilde{\psi}$  so that  $\tilde{\psi} = \tan^{-1}[(\beta b/c)\cos \theta]$ . Hence, the traces through the 50-percent chord at the wing tip and the  $\xi$  axis (see lines XX and YY in fig. 2(a)) define a longitudinal distance  $|(\beta b/c)\cos \theta|$ . In accordance with reference 4 the sheared configurations are formed by shearing each element of the upper wing panel a distance  $|(\beta b/c)\cos \theta|\eta$  forward and shearing each element of the lower wing panel a distance  $|(\beta b/c)\cos \theta|\eta$  rearward for  $0 \leq \theta < \pi/2$  (see the dashed lines in fig. 2(a)). For  $\theta = \pi/2$ , the sheared and given configurations are identical. For  $\pi/2 < \theta \leq \pi$ , the upper and lower wing panels are sheared rearward and forward, respectively. However, in view of symmetry of a pair of wing panels only the values of  $0 \leq \theta \leq \pi/2$  are considered.

Within the slenderness requirements of the supersonic area rule (see the METHOD section), the normal cross-sectional area distribution of the sheared configurations is identical to the frontal projection of the area distribution intercepted on the given configuration by the oblique planes. From figure 2(a) it is seen that the tangent of the sweep angle of the 50-percent chord line of the upper and lower sheared wing panels can be defined by

$$\left. \begin{aligned} K_U &= K_O - \beta \frac{b}{c} \cos \theta \\ K_L &= K_O + \beta \frac{b}{c} \cos \theta \end{aligned} \right\} \quad (B1)$$

Addition of the two parts of equation (B1) yields the following relation for the upper and lower wing panels.

$$K_L + K_U = 2K_O \quad (B2)$$

Thus, for a given  $\beta$  and  $\theta$  the sheared wing panels are related to the proper equivalent bodies of revolution by the single parameter  $K$ .

Exposed wings.- The exposed wing panels of a wing-body combination are shown in dimensionless coordinates in figure 2(b). Since these wing panels are made dimensionless with respect to conditions at the wing-body juncture (see appendix A), it is convenient to consider a separate coordinate system for the upper and lower exposed wing panels. The  $\xi$  axes of these separate coordinate systems are separated in the spanwise direction by a distance  $2\eta_1$  (see fig. 2(b)). The distance  $\eta_1$  is the ratio of the body radius at the averaged wing-body juncture to the semi-span of the exposed wing panels. With respect to the coordinate system of the complete wing, the semispan of the complete plan form is  $1 + \eta_1$ . Hence, the trace XX in figure 2(b) through the 50-percent chord at the wing tip and the  $\xi$  axis defines a longitudinal distance  $|(\beta b_1/c_1)\cos \theta|(1 + \eta_1)$ . The sheared configurations of the exposed wing panels are formed by shearing the plan form as before. As the exposed wing panels are sheared with respect to origin of the complete wing (O in fig. 2(b)), the origins of the coordinate systems of the separate exposed wing panels become longitudinally separated a distance  $\Delta = 2|(\beta b_1/c_1)\cos \theta|\eta_1$  as shown by the dashed lines in figure 2(b). The origin of each panel is translated, in opposite directions, a distance  $|(\beta b_1/c_1)\cos \theta|\eta_1$ . Since  $b_1/c_1 = b/c$  for plan forms with straight leading and trailing edges, it can be determined with the aid of figure 2(b) that equation (B1) also serves to identify the sheared exposed wing panels with the proper equivalent bodies of revolutions when the equations are applied relative to the individual coordinate system of each exposed wing panel.

The value of identifying the sheared wing panels with the parameter  $K$  rather than with  $\beta$  and  $\theta$  was first demonstrated in reference 4. In reference 4 it was found possible to calculate the area distribution of the sheared wing panels as a function of  $\xi$ ,  $K$ , and fixed geometric properties of the given plan form. As shown in appendix C of this report, the moments and lengths of the sheared wing panels can also be calculated as a function of  $K$  and fixed geometric properties of the given plan form.

### Tails

The shearing concept described above for exposed wings is also applicable to the exposed portion of tails when the tails are rendered dimensionless with respect to conditions at the tail-body juncture. The proper values of  $K$  for horizontal tails are determined from equation (B1) with  $\theta_{HT} = \theta_W$ . For vertical tails either part of equation (B1) is used with  $\theta_{VT} = \theta_W + \pi/2$ . The sheared configurations for vertical tails are symmetrical in  $\pi$  rather than  $\pi/2$ .

### PAIRS OF BODIES OF REVOLUTION

A pair of bodies of revolution is shown in dimensionless coordinates by the solid lines in figure 3. The configuration is rendered dimensionless with respect to the larger body, E, and the lateral distance between the bodies,  $d$ . If the origin of the coordinate system is chosen at the center of body E, traces in the  $\xi, \eta$  plane made by the intersections of the oblique planes and the  $\xi, \eta$  plane are inclined to the  $\eta$  axis at an angle  $\tilde{\omega}$  so that  $\tilde{\omega} = \tan^{-1}[(\beta d/l_E)\cos\theta]$ . Similar to the case of sheared wings, each element of body H is sheared a distance  $|(\beta d/l_E)\cos\theta|$ . Sheared configurations for a pair of bodies of revolution are symmetrical in  $\pi$ . Hence, for  $0 \leq \theta < \pi/2$  body H is sheared rearward. For  $\theta = \pi/2$  the sheared and given configurations are identical. For  $\pi/2 < \theta \leq \pi$  body H is sheared forward as shown by the dashed lines in figure 3. For a given  $\beta$  and  $\theta$  the sheared configurations can be related to the proper equivalent bodies of revolution by the single parameter  $\tilde{\delta}$  which indicates the longitudinal separation of the centers of the sheared bodies; that is,

$$\tilde{\delta} = \tilde{\delta}_0 + \beta \frac{d}{l_E} \cos \theta \quad (B3)$$

where  $\tilde{\delta}_0$  is the longitudinal distance, in dimensionless coordinates, between the centers of the given bodies (see fig. 3).

## APPENDIX C

MOMENTS AND LENGTHS FOR SHEARED WINGS  
AND TAILS

Zero-lift wave-drag calculations by the present method require a knowledge of the moments and lengths of the various components and pairs of components of a series of equivalent bodies of revolution (or sheared configurations). As mentioned in the METHOD section, the moments and lengths of slender-body-of-revolution components alone are relatively simple to determine because the area distribution of the sheared components are independent of Mach plane orientation. The lengths of pairs of these components are also relatively simple to determine, since, as shown in appendix B, the effect of changes in  $\theta$  on the sheared configurations of such components is merely one of translation of one body (see fig. 3). The area distribution of sheared wing and tail components, on the other hand, is dependent upon  $\theta$ . Consequently, the moments and lengths required are more difficult to determine. Therefore, this appendix presents a technique for determining the moments and lengths of wings and tails required by the present method to calculate the zero-lift wave drag of each panel alone plus the interference between panels.

In the following analysis, use of the term "wing(s)" will be construed to include both wings and tails. Application of the results to tails is made merely by means of the proper value of  $K$  for the tails as previously described in appendix B.

The results of the following analyses are applicable to a large yet restricted group of wings. This group satisfies the following conditions:

- i. The spanwise variation of the 50-percent chord line is linear,
- ii. The boundaries of the plan form, the spanwise variation of the local chord, and the spanwise variation of the thickness along lines of constant percent chord can be expressed analytically.
- iii. The wing has the same airfoil section at all spanwise stations; that is, only spanwise variations in thickness and/or thickness ratio are allowed.

Condition (iii) can be relaxed to include wings with one airfoil section out to a discontinuity in plan form, for example, a fence or extended leading edge, and a different airfoil section from the discontinuity out to the wing tip. In such cases, each portion of the plan form is treated as a separate entity.

This appendix presents the results only for trapezoidal plan forms with taper ratios from 0 to 1. Moments and lengths for other plan forms, such as an elliptic plan-form wing can be obtained by following the same technique presented herein and inserting the proper analytical expressions for the plan form and the spanwise variation of the local chord (or half-chord).

MOMENTS AND LENGTHS FOR THE CALCULATION  
OF THE DRAG OF ONE WING PANEL

Moments

The sheared plan form of one exposed wing panel of a wing-body combination is shown in dimensionless coordinates in figure 4. As shown in appendix A, the moments of one sheared wing panel can be expressed as

$$\tilde{M}_{ok} \left( \beta \frac{b}{c}, \theta \right) = \frac{2}{\pi} \int_{\eta=0}^1 \int_{\xi=-\tilde{l}(\beta b/c, \theta)}^{\tilde{l}(\beta b/c, \theta)} \tau \left( \xi, \eta, \beta \frac{b}{c}, \theta \right) \xi^k d\xi d\eta \quad (C1)$$

It will be recalled that this definition requires that the moments be calculated about the midpoint of the total length of the sheared wing panel. It has been found expedient to calculate first the moments about the axis through the origin of the coordinate system shown in figure 4 ( $\xi = 0$ ) and then transfer these moments, designated  $\tilde{M}'_{ok}(\beta b/c, \theta)$ , to an axis through the midpoint of the total length. Thus

$$\tilde{M}'_{ok} \left( \beta \frac{b}{c}, \theta \right) = \frac{2}{\pi} \int_{\eta=0}^1 \int_{\xi=\xi_1(\beta b/c, \theta, \eta)}^{\xi_2(\beta b/c, \theta, \eta)} \tau \left( \xi, \eta, \beta \frac{b}{c}, \theta \right) \xi^k d\xi d\eta \quad (C2)$$

where  $\xi_1(\beta b/c, \theta, \eta)$  and  $\xi_2(\beta b/c, \theta, \eta)$  are functions which define the leading and trailing edges of the sheared plan form, respectively. Equation (C2) can be simplified somewhat by replacing the combined variables  $\beta b/c$  and  $\theta$  by the single parameter  $K$  ( $K_U$  or  $K_L$ ) as described in the METHOD section (see eq. (25)). Hence,

$$\tilde{M}'_{ok}(K) = \frac{2}{\pi} \int_{\eta=0}^1 \int_{\xi=\xi_1(K, \eta)}^{\xi_2(K, \eta)} \tau(\xi, \eta, K) \xi^k d\xi d\eta \quad (C3)$$

As shown in appendix C of reference 4, the plan-form dimensionless thickness distribution for plan forms satisfying the above mentioned restrictions can be written

$$\tau(\xi, \eta, K) = \Phi(\eta) \tau[\alpha(\xi, \eta, K)] \quad (C4)$$

where  $\Phi(\eta)$  is the spanwise variation of the dimensionless thickness along lines of constant percent chord,  $\tau[\alpha(\xi, \eta, K)]$  is the local airfoil section dimensionless thickness along lines of constant percent chord, and  $\alpha(\xi, \eta, K)$  defines lines of constant percent chord. In other words, the function  $\alpha(\xi, \eta, K)$  expresses any point  $\xi, \eta$  in any sheared plan form (for any value of  $K$ ) as the chord station of the local dimensionless airfoil section. The chord station is measured relative to the local 50-percent chord as indicated by

$$\alpha(\xi, \eta, K) = \alpha = \frac{\xi - K\eta}{\tilde{c}(\eta)} ; \quad -1 \leq \alpha \leq 1 \quad (C5)$$

In equation (C5)  $\tilde{c}(\eta)$  is the spanwise variation of the local dimensionless half-chord, which, for the plan forms considered herein, is given by

$$\tilde{c}(\eta) = 1 - B\eta \quad (C6)$$

In equation (C6)

$$B = 1 - \lambda_1 \quad (C7)$$

and  $\lambda_1$  is the taper ratio of the exposed wing panel. From equations (C5) to (C7) equation (C4) can be written

$$\tau(\xi, \eta, K) = \Phi(\eta) \tau(\alpha) \quad (C8)$$

where

$$\alpha = \frac{\xi - K\eta}{1 - B\eta} ; \quad -1 \leq \alpha \leq 1 \quad (C9)$$

Substituting equations (C8) and (C9) and the equations for  $\xi_1(K, \eta)$  and  $\xi_2(K, \eta)$  (see fig. 4) in equation (C3), making a change of variable from  $\xi$  to  $\alpha$ , and first performing the integration with respect to  $\alpha$  yields

$$\tilde{M}_{ok}'(K) = \int_{\eta=0}^1 \Phi(\eta) \frac{2}{\pi} \int_{\alpha=-1}^1 \tau(\alpha) [K\eta + (1-B\eta)\alpha]^k (1-B\eta) d\alpha d\eta \quad (C10)$$

Now

$$[K\eta + (1-B\eta)\alpha]^k = \sum_{m=0}^k C_m^k (K\eta)^{k-m} (1-B\eta)^m \alpha^m$$

where

$$C_m^k = \frac{k!}{(k-m)!m!}$$

Hence, equation (C10) becomes

$$\tilde{M}_{Ok}'(K) = \sum_{m=0}^k C_m^k K^{k-m} \frac{2}{\pi} \int_{\alpha=-1}^1 \tau(\alpha) \alpha^m d\alpha \cdot \int_{\eta=0}^1 \eta^{k-m} (1-B\eta)^{m+1} \phi(\eta) d\eta \quad (C11)$$

Let

$$I_m = \frac{2}{\pi} \int_{\alpha=-1}^1 \tau(\alpha) \alpha^m d\alpha \quad (C12)$$

and since

$$(1-B\eta)^{m+1} = \sum_{r=0}^{m+1} (-1)^r C_r^{m+1} B^r \eta^r$$

equation (C11) becomes

$$\tilde{M}_{Ok}'(K) = \sum_{m=0}^k C_m^k K^{k-m} I_m \sum_{r=0}^{m+1} (-1)^r C_r^{m+1} B^r \int_{\eta=0}^1 \eta^{k-m+r} \phi(\eta) d\eta \quad (C13)$$

Let

$$E_{k-m+r} = \int_{\eta=0}^1 \eta^{k-m+r} \phi(\eta) d\eta \quad (C14)$$

Then

$$\tilde{M}_{Ok}'(K) = \sum_{m=0}^k C_m^k K^{k-m} \sum_{r=0}^{m+1} (-1)^r C_r^{m+1} B^r E_{k-m+r} I_m$$

Finally, if

$$F_{km} = \sum_{r=0}^{m+1} (-1)^r C_r^{m+1} B^r E_{k-m+r} \quad (C15)$$

the moments about the axis through the origin of the coordinate system of the sheared wing panel ( $\xi = 0$ ) are given by

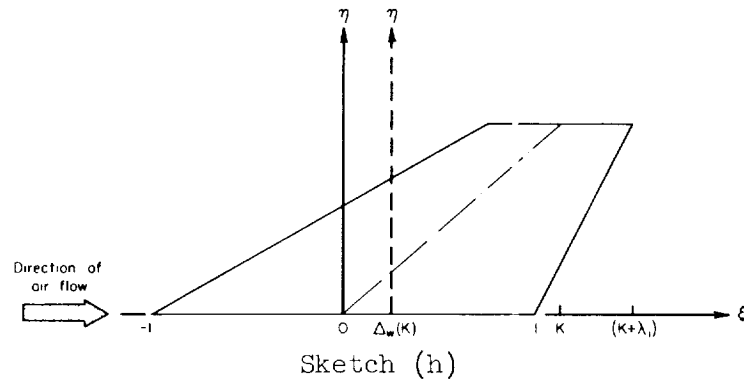
$$\tilde{M}_{ok}'(K) = \sum_{m=0}^k C_m^k K^{k-m} F_{km} I_m \quad (C16)$$

The physical interpretation of equation (C16) is that the moments are functions of the single parameter  $K$ , which identifies the sheared wing panel, and the geometric properties of the given wing panel. As indicated by equation (C15),  $F_{km}$  is a function of the taper ratio of the given wing panel and the spanwise variation of the dimensionless thickness of the given wing panel along lines of constant percent chord; that is,  $\lambda_1$  enters through  $B$  (see eq. (C7)) and  $\phi(\eta)$  enters through  $E_{k-m+r}$  (see eq. (C14)). It should be recalled (see restrictive condition (ii) above) that  $\phi(\eta)$  is a known analytical expression; therefore,  $E_{k-m+r}$  can always be evaluated with little or no difficulty. Several practical examples of  $\phi(\eta)$  are tabulated below for the plan forms discussed herein.

Thickness characteristic	$\phi(\eta)$	Definition of constants
Constant thickness ratio	$1-B\eta$	$B$ (see eq. (C7))
Linear variation in thickness ratio	$(1-B\eta)(1-G\eta)$	$G = 1 - \frac{\text{thickness ratio at } \eta=1}{\text{thickness ratio at } \eta=0}$
Linear variation in thickness	$1-H\eta$	$H = 1 - \frac{\text{thickness at } \eta=1}{\text{thickness at } \eta=0}$

The quantities  $I_m$  are integral functions of the dimensionless airfoil-section thickness distribution,  $\tau(\alpha)$  (see eq. (C12)). When  $\tau(\alpha)$  is known analytically  $I_m$  can also be evaluated with little or no difficulty. Generally, however, an analytical expression for  $\tau(\alpha)$  may not be available. In these instances the evaluation of equation (C12) requires special treatment. A simplified technique for finding  $I_m$  for airfoil sections with a nonanalytic thickness distribution is presented in appendix E.

It remains to transfer the moments from the axis through  $\xi = 0$  to an axis through the midpoint of the total length of the wing panel. With the aid of sketch (h) it is seen that such an axis passes through



$\xi = \Delta_W(K)$  where  $\Delta_W(K)$  indicates the moment transfer distance (and direction relative to the axis through  $\xi = 0$ ) for a sheared wing panel alone. The analytical expression for the moments calculated about the  $\xi = \Delta_W(K)$  axis is

$$\tilde{M}_{Ok}(K) = \frac{2}{\pi} \int_{\eta} \int_{\xi} \tau(\xi, \eta, K) [\xi - \Delta_W(K)]^k d\xi d\eta \quad (C17)$$

Since

$$[\xi - \Delta_W(K)]^k = \sum_{s=0}^k (-1)^s C_s^k \xi^{k-s} [\Delta_W(K)]^s$$

equation (C17) can be written

$$\tilde{M}_{Ok}(K) = \sum_{s=0}^k (-1)^s C_s^k [\Delta_W(K)]^s \frac{2}{\pi} \int_{\eta} \int_{\xi} \tau(\xi, \eta, K) \xi^{k-s} d\xi d\eta \quad (C18)$$

By definition from equation (C3)

$$M'_{O(k-s)}(K) = \frac{2}{\pi} \int_{\eta} \int_{\xi} \tau(\xi, \eta, K) \xi^{k-s} d\xi d\eta$$

which defines moments about the  $\xi = 0$  axis. Therefore, moments about the  $\xi = \Delta_W(K)$  axis are given as a function of the moments about the  $\xi = 0$  axis as

$$\tilde{M}_{ok}(K) = \sum_{s=0}^k (-1)^s c_s^k [\Delta_W(K)]^s \tilde{M}_{o(k-s)}(K) \quad (C19)$$

Values of  $\Delta_W(K)$  for various values of  $K$  cannot, of course, be determined until the total length of the sheared wing panel,  $l_W(K)$ , is known. Therefore,  $\Delta_W(K)$  is evaluated in the following paragraph in conjunction with the evaluation of  $l_W(K)$ .

#### Lengths and Moment Transfer Distances

The analytical expressions for the total length and moment transfer distance for each sheared wing panel alone have different forms depending upon the value of  $K$  relative to  $B$ . Sheared wing panels for ranges of  $K < -B$ ,  $-B \leq K \leq B$ , and  $K > B$  are shown in figure 5. Consider the sheared wing panel for  $K > B$  shown in figure 5(c). Actually the length ratio  $[c/l(K)]_W$  or  $[\tilde{c}/\tilde{l}(K)]_W$  is of interest. From figure 5(c)

$$\tilde{l}_W(K) = 1 + (K+\lambda_1) \quad (C20)$$

and

$$\Delta_W(K) = (K+\lambda_1) - \frac{1}{2} \tilde{l}_W(K)$$

which, from equations (C7) and (C20), becomes

$$\Delta_W(K) = \frac{1}{2} (K-B) \quad (C21)$$

Since  $\tilde{c} = 2$ , from equation (C20)

$$\left[ \frac{c}{l(K)} \right]_W = \frac{2}{1+(K+\lambda_1)}$$

which, from equations (C7) and (C21), can be written

$$\left[ \frac{c}{l(K)} \right]_W = \frac{1}{1+\Delta_W(K)} \quad (C22)$$

In a similar manner  $\Delta_W(K)$  and  $[c/l(K)]_W$  can be determined for the ranges of  $K$  defined by the sheared wing panels in figures 5(a) and 5(b). The results are tabulated below:

Moment transfer distances and length ratios for sheared wing panels alone			
Sheared wing panel, $K$ range	$K < -B$	$-B \leq K \leq B$	$K > B$
$\Delta_W(K)$	$(1/2)(K+B)$	0	$(1/2)(K-B)$
$\left[ \frac{c}{l(K)} \right]_W$	$\frac{1}{1-\Delta_W(K)}$	1	$\frac{1}{1+\Delta_W(K)}$

#### MOMENTS AND LENGTHS FOR THE CALCULATION OF INTERFERENCE DRAG BETWEEN WING PANELS

##### Moments

Moments for the upper and lower sheared wing panels used in the interference calculations are determined in the same general manner as in the case of the drag calculations for one sheared wing panel alone. The moments used in the drag calculations for one sheared wing panel alone which were calculated about the  $\xi = 0$  axis by equation (C16) can also be used in the interference calculations to obtain the moments about the midpoint of the total length of the combined sheared wing panels. Values of  $\tilde{M}_{Ok}'(K)$  are selected for the upper and lower wing panels in the ordered pairs indicated by equation (31). These moments, in conjunction with the respective upper and lower transfer distances for the interference calculations,  $\Delta_{IU}(K)$  and  $\Delta_{IL}(K)$ , are used in equation (C19) to obtain values of  $\tilde{M}_{Ok}(K)$  for interference. The actual transfer distances are, again, dependent upon the combined length of both sheared wing panels.

##### Lengths and Moment Transfer Distances

The analytical expressions for the total length of both wing panels and the separate moment transfer distance for each wing panel used in the interference calculations for a sheared plan form have different forms

depending upon the value of  $K_O$  relative to  $B$  and upon the value of  $K_L$  relative to  $K_O$  and to  $B$ . Sheared plan forms defining the ranges of critical values of  $K_O$ ,  $B$ , and  $K_L$  are shown in figure 6.

Rather than express  $\Delta(K)$ ,  $\Delta_{IU}(K)$ ,  $\Delta_{IL}(K)$ , and  $[c/l(K)]_I$  as a function of  $K_U$  and  $K_L$ , it has been found convenient to make use of the relationship between  $K_U$  and  $K_L$  given by equation (31) and express all quantities as a function of  $K_L$ . For all the sheared plan forms of figure 6

$$\Delta(K) = \eta_1(K_L - K_U)$$

but from equation (31) one can write

$$\Delta(K) = 2\eta_1(K_L - K_O) \quad (C23)$$

Consider the plan forms shown in figure 6(e) for  $K_O > B$  and  $K_L > (B + 2K_O)$ . From the figure

$$\tilde{l}_I(K) = (K_L + \lambda_1) + \Delta(K) - (K_U - \lambda_1) \quad (C24)$$

$$\Delta_{IU}(K) = \frac{1}{2} \tilde{l}_I(K) + (K_U - \lambda_1) \quad (C25)$$

$$\Delta_{IL}(K) = (K_L + \lambda_1) - \frac{1}{2} \tilde{l}_I(K) \quad (C26)$$

From equation (31) equations (C24) to (C26) become

$$\tilde{l}_I(K) = 2(K_L - K_O + \lambda_1) + \Delta(K) \quad (C27)$$

$$\Delta_{IU}(K) = \frac{1}{2} [2K_O + \Delta(K)] \quad (C28)$$

$$\Delta_{IL}(K) = \frac{1}{2} [2K_O - \Delta(K)] \quad (C29)$$

Finally, since  $\tilde{c} = 2$

$$\left[ \frac{c}{l(K)} \right]_I = \frac{1}{K_L - K_O + \lambda_1 + \frac{1}{2} \Delta(K)} \quad (C30)$$

In a similar manner  $\Delta_{IU}(K)$ ,  $\Delta_{IL}(K)$ , and  $[c/l(K)]_I$  can be determined for the ranges of critical values of  $K_O$ ,  $B$ , and  $K_L$  defined by the other sheared plan forms in figure 6. The results are tabulated below:

Moment transfer distances and length ratios for the interference between wing panels of sheared plan forms			
Given plan form, $K_O$ range	$0 \leq K_O \leq B$	$0 \leq K_O \leq B$ and $K_O > B$	$0 \leq K_O \leq B$ and $K_O > B$
Sheared plan form, $K_L$ range	$K_O \leq K_L \leq B$	$B^* \leq K_L \leq (B+2K_O)$	$K_L > (B+2K_O)$
$\Delta_{IU}(K)$	$(1/2)\Delta(K)$	$(1/2)[K_L-B+\Delta(K)]$	$(1/2)[2K_O+\Delta(K)]$
$\Delta_{IL}(K)$	$-(1/2)\Delta(K)$	$(1/2)[K_L-B-\Delta(K)]$	$(1/2)[2K_O-\Delta(K)]$
$\left[ \frac{c}{l(K)} \right]_I$	$\frac{1}{1+(1/2)\Delta(K)}$	$\frac{1}{(1/2)[K_L+\lambda_1+1+\Delta(K)]}$	$\frac{1}{K_L-K_O+\lambda_1+(1/2)\Delta(K)}$
Limiting values for the $K_U$ range for sheared plan forms can be determined from the relation: $K_L + K_U = 2K_O$			
$\Delta(K) = \eta_1(K_L-K_U) = 2\eta_1(K_L-K_O)$			

\*For  $K_O > B$  the lower limit  $B$  is replaced by  $K_O$ .

## APPENDIX D

## SAMPLE CALCULATIONS

Sample calculations of the dimensionless zero-lift wave drag for several of the configurations discussed in this report are presented in order to demonstrate the computing procedure in detail. From equations (A3) to (A9) the general computing procedure can be stated as follows.

To calculate the drag contribution of each component or the interference between each pair of components of an equivalent body of revolution

1. Determine the total length of each component or of each pair of components and calculate the moments about the midpoint of this length.

2. Calculate the length ratios for each component or pair of components.

3. With the information of steps 1 and 2 calculate the quantities  $\tilde{L}_{no}(\beta b/c, \theta)$  (see eq. (A4)).

4. With the information of step 3 it is a simple matter to evaluate equations (A5) and (A7), the latter of which represents the dimensionless zero-lift wave-drag contribution of one equivalent body.

5. The results of step 4 for all equivalent bodies are then graphically averaged according to equation (A9) to obtain the dimensionless zero-lift wave drag of each configuration component alone or the interference between components, as the case may be.

If desired, the results of step 4 for the drag of each component and the interference between components may be summed before undertaking step 5. Dimensional values are obtained, of course, by evaluating the coefficients of equations (A11) or (A16) for airplane configurations or systems of bodies of revolution, respectively.

## SINGLE BODY OF REVOLUTION

From equation (34) the dimensionless area distribution of a Sears-Haack body can be written

$$\tilde{S}(\xi) = (1-\xi^2)^{\frac{3}{2}} \quad (D1)$$

The total length is that of the body. Using equation (D1) in equation (A17) the moments are calculated to be

k	$\tilde{M}_{Ok}$	k	$\tilde{M}_{Ok}$
0	3/4	1	0
2	1/8	3	0
4	3/64	5	0
6	3/128	7	0

For a single body alone the length ratio is unity. Hence, from equation (A17)

$$\tilde{L}_{20} = 3/4$$

and all other  $\tilde{L}_{n0} \equiv 0$  for  $n > 2$ . Therefore, from equations (22) and (21), the dimensionless zero-lift wave drag at Mach number 1 is

$$\tilde{D} = 2(3/4)^2 = 9/8 = 1.125 \quad (D2)$$

#### PAIR OF BODIES OF REVOLUTION

The total zero-lift wave drag will be calculated for the pair of Sears-Hauck bodies shown in sketch (g) for only  $M = 1$ , since these calculations are typical of those for each equivalent body required for  $M > 1$ . The total zero-lift wave drag for  $M = 1$  is given by (see eq. (26))

$$\tilde{D}_T = \tilde{D}_E + \tilde{D}_H + \tilde{D}_{EH} \quad (D3)$$

The first two terms of equation (D3), respectively, represent the drag contributions of bodies E and H alone and are given by equation (D2).

In evaluating the interference term,  $\tilde{D}_{EH}$ , the dimensionless value of the combined length of both bodies is 4. The moments of each body about an axis through the origin (see above table for single body of revolution) must be transferred to an axis through the midpoint of the total length. It can be seen from sketch (g) that such an axis passes through the tail of body E and the nose of body H. Hence, in dimensionless coordinates, the transfer distances are

$$\left. \begin{aligned} \Delta_E &= 1 \\ \Delta_H &= -1 \end{aligned} \right\} \quad (D4)$$

for bodies E and H, respectively. From equation (D4) and from use of the moments calculated above for a single body of revolution as values of  $\tilde{M}_{ok}'$ , equation (C19) yields the following moments about the midpoint of the total length of both bodies.

k	$\tilde{M}_{ok}$	k	$\tilde{M}_{ok}$
0	3/4	1	$\mp$ 3/4
2	7/8	3	$\mp$ 9/8
4	99/64	5	$\mp$ 143/64
6	429/128	7	$\mp$ 663/128
(-) for odd k is for body E			

The ratio of the length of each individual body to the total length of bodies is 1/2. Hence, from equation (A17) the quantities  $\tilde{L}_{no}$  for both bodies are

n	$\tilde{L}_{no}$	n	$\tilde{L}_{no}$
2	3/4	3	$\mp$ 3/2
4	9/8	5	0
6	-33/64	7	$\pm$ 3/32
8	39/128	9	$\mp$ 3/32
Upper sign for odd n is for body E			

Using the above information in equations (28) and (27) yields

$$\tilde{D}_{EH} = 0.204 \quad (D5)$$

Finally, from use of equations (D2) and (D3) in equation (D3), the dimensionless total zero-lift wave drag is

$$\tilde{D}_T = 2.454$$

#### COMPLETE WING

Calculations of the dimensionless zero-lift wave drag are presented for a family of diamond plan-form wings (see sketch (b)) which have biconvex airfoil sections of constant thickness ratio. Calculations have been made for a Mach number range corresponding to values of  $\beta b/c$  from 0 to 3.

The important dimensionless quantities describing the plan form, the airfoil section, and the spanwise variation of the thickness along lines of constant percent chord are given, respectively, by

$$K_0 = \lambda = 0 ; \quad B = 1 \quad (D6)$$

$$\tau(\alpha) = 1 - \alpha^2 \quad (D7)$$

$$\Phi(\eta) = 1 - \eta \quad (D8)$$

The value of  $\tau(\alpha)$  given by equation (D7) is actually for a parabolic-arc airfoil section. However, for values of the thickness ratio up to about 5 percent, this is a satisfactory approximation.

#### Calculations for the Wave Drag of Each Wing Panel Alone

Initially one determines the range of values of  $K$  for which the calculations are to be made. Since  $K_0 = 0$  and  $(\beta b/c)_{\max} = 3$ , the range of the values of  $K$  for which the moments of one wing panel must be calculated are determined from equation (25) as  $K_{U_{\min}} = -3$  and  $K_{L_{\max}} = 3$ .

The moments of each sheared wing panel are first calculated about the 50-percent chord line at the plane of symmetry. From equations (CL4) and (D7)

$$I_m = \frac{2}{\pi} \int_{-1}^1 (1-\alpha^2)\alpha^m d\alpha$$

$$I_m = \begin{cases} \frac{4}{\pi} \left( \frac{1}{m+1} - \frac{1}{m+3} \right) ; & m \text{ even} \\ 0 & ; m \text{ odd} \end{cases} \quad (D9)$$

Values of  $0 \leq m \leq 7$  are required.

From equations (CL4) and (D8)

$$E_{k-m+r} = \int_0^1 (1-\eta)\eta^{k-m+r} d\eta$$

$$E_{k-m+r} = \frac{1}{k-m+r+1} - \frac{1}{k-m+r+2} \quad (D10)$$

Values of  $0 \leq (k-m+r) \leq 8$  are required. From use of the results of equation (D10) in equation (C15) values of  $F_{km}$  are determined for  $0 \leq k \leq 7$  and  $0 \leq m \leq k$ . With  $F_{km}$  and  $I_m$  determined, moments about the  $\xi = 0$  axis are determined for the sheared wing panels by use of the desired values of  $-3 \leq K \leq 3$  in equation (C16). Because the airfoil section is symmetrical about the 50-percent chord, in this case

$$\left. \begin{aligned} \tilde{M}_{Ok}'(-K) &= \tilde{M}_{Ok}'(K) && \text{for } k \text{ even} \\ \tilde{M}_{Ok}'(-K) &= -\tilde{M}_{Ok}'(K) && \text{for } k \text{ odd} \end{aligned} \right\} \quad (D11)$$

Thus, only values of  $0 \leq K \leq 3$  are necessary.

Next, the moment of each sheared wing panel alone must be transferred to an axis through the midpoint of the total length of each sheared wing panel. From the table of appendix C for the sheared wing panels alone, the transfer distances and length ratios are

K range	$\Delta_W(K)$	$[c/l(K)]_W$
$K < -1$	$(1/2)(K+1)$	$2/(1-K)$
$-1 \leq K \leq 1$	0	1
$K > 1$	$(1/2)(K-1)$	$2/(1+K)$

With the above values of  $\Delta_W(K)$  and the values of  $\tilde{M}_{Ok}'(K)$ , values of  $\tilde{M}_{Ok}(K)$  are determined from equation (C19) for  $0 \leq k \leq 7$ . For this special case, the relationships of equation (D11) also apply to the moments about the midpoint of the total length of each sheared wing panel. With the information now available the dimensionless zero-lift wave drag of the upper and lower sheared wing panels alone can be calculated from equations (23), (22), and (21) for  $2 \leq n \leq 9$ . The results are plotted in figure 7 as a function of  $K$ . It will be noted that for this case,  $\tilde{D}_W(K)$  is symmetrical about  $K = 0$ . This is again the result of the symmetrical airfoil section. In view of the relationships of equation (D11) it can be seen from equation (A17) that

$$\left. \begin{aligned} \tilde{L}_{no}(-K) &= \tilde{L}_{no}(K) && \text{for } n \text{ even} \\ \tilde{L}_{no}(-K) &= -\tilde{L}_{no}(K) && \text{for } n \text{ odd} \end{aligned} \right\} \quad (D12)$$

Since  $[\tilde{L}_{no}(K)]^2$  is required (see eq. (22)) and the length ratios are symmetrical about  $K = 0$ ,  $\tilde{D}_W(K)$  is necessarily symmetrical about  $K = 0$ .

## Calculations for the Interference Wave Drag Between Wing Panels

To calculate the interference between wing panels the ordered pairs of upper and lower sheared wing panels are first determined from equation (31); thus

$$K_U = -K_L \quad (D13)$$

The moments,  $\tilde{M}_{Ok}'(K)$ , for the ordered pairs of sheared wing panels must be transferred to the midpoint of the total length of both sheared wing panels. From the table in appendix C for interference between sheared wing panels, the transfer distances and length ratios are

$K_L$ range	$\Delta_{IU}(K)$	$\Delta_{IL}(K)$	$[c/l(K)]_I$
$0 \leq K_L \leq 1$	0	0	1
$K_L > 1$	0	0	$1/K_L$

From equations (29) and (30), values of  $\tilde{I}_{no}(K)$  are calculated for the pairs of upper and lower sheared wing panels for  $2 \leq n \leq 9$ . Again, as a result of the symmetry of the given configuration, use of equation (D13) in equation (D12) indicates that the detailed calculations of values of  $\tilde{I}_{no}(K)$  for interference are necessary for only the lower sheared wing panels. The dimensionless interference zero-lift wave drag between sheared wing panels is given by equations (28) and (27). The results are plotted directly as a function of  $\beta b/c \cos \theta$  in figure 8. Also shown in figure 8 are the dimensionless zero-lift wave-drag results for each of the sheared wing panels alone replotted as a function of  $\beta b/c \cos \theta$  from the data of figure 7. It is emphasized that all results shown in figures 7 and 8 were calculated using six significant figures.

## Calculations for the Total Wave Drag of the Complete Wing

The total zero-lift wave drag for each complete sheared configuration is calculated using the form of equation (26) for an equivalent body. The results are included in figure 8. The variation of the dimensionless total zero-lift wave drag of the complete wings with  $\beta b/c$  is obtained by replotting the total wave-drag results of figure 8 against  $\theta$ , for constant values of  $\beta b/c$ , and graphically averaging the results as indicated by equation (20). It should be recalled, however, that complete plan forms are symmetrical in  $\pi/2$ . Values of  $\tilde{D}_T(\beta b/c, \theta)$  obtained from the data of figure 8 for several values of  $\beta b/c$  are shown in figure 9 replotted against  $\theta$ . The dimensionless total zero-lift wave-drag results,  $\tilde{D}_T(\beta b/c)$ , are shown in figure 10.

The data of figure 1(a) were obtained from use of the results of figure 10 in equation (33). For this complete plan form  $b_1/b = \tau_1/\tau = 1$ .

## APPENDIX E

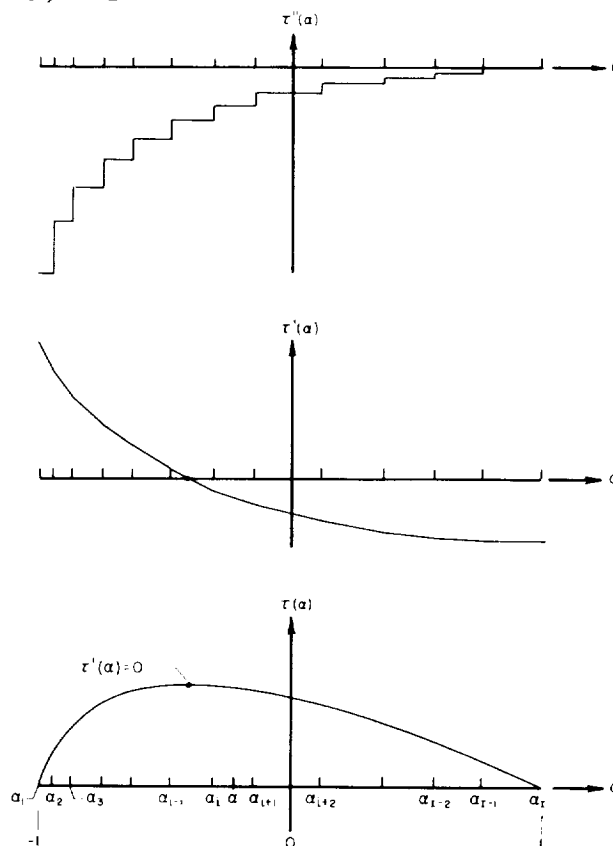
EVALUATION OF THE INTEGRAL FUNCTIONS FOR AIRFOIL SECTIONS  
WITH NONANALYTIC THICKNESS DISTRIBUTIONS

Determination of the moments used in the zero-lift wave-drag calculations depends upon the evaluation of the integral functions of the airfoil-section thickness distribution given in appendix C by

$$I_m = \frac{2}{\pi} \int_{-1}^1 \tau(\alpha) \alpha^m d\alpha \quad (C12)$$

where  $\tau(\alpha)$  is the dimensionless airfoil-section thickness distribution for  $-1 \leq \alpha \leq 1$ . Equation (C12) can be evaluated with little or no difficulty for airfoil sections for which an analytical expression for  $\tau(\alpha)$  is available, such as an NACA four-digit series airfoil section. The thickness distribution is not available in analytical form for many airfoil sections, such as an NACA six-digit series airfoil section. The thickness is generally specified, however, at about 20 airfoil chord stations. It appears, therefore, that a graphical evaluation of equation (C12) is possible. Unfortunately, experience has demonstrated that the accuracy of such a technique is insufficient to provide reliable wave-drag results. Consequently, special techniques are required to obtain an approximate expression for the thickness distribution of an arbitrary airfoil section, and hence, evaluate equation (C12) analytically.

In appendix C of reference 4 it was found possible to approximate the thickness distribution of an arbitrary airfoil section in analytical form with a series of adjacent parabolic-arc segments of continuous slope. This is possible when the airfoil-section thickness is specified at a sufficient number of chord stations, say  $I$ , to define adequately the thickness distribution, and the slope of the thickness distribution is given for at least one chord station (see the lower part of sketch (i)). The salient feature of this type of approximation which is important to the evaluation of equation (C12)



Sketch (i)

is the fact that the second derivative of the thickness distribution is constant over each segment of parabolic arc (see the upper part of sketch (i)). Hence, one may write for the second derivative of the dimensionless thickness distribution

$$\tau''(\alpha) \approx \tau''(\alpha_i) = \text{constant for } \left\{ \begin{array}{l} \alpha_i \leq \alpha < \alpha_{i+1} \\ 1 \leq i \leq (I-1) \end{array} \right\} \quad (\text{E1})$$

The details for finding the analytical expression for  $\tau(\alpha)$ ,  $\tau'(\alpha)$ , and  $\tau''(\alpha)$  can be found in appendix C of reference 4. With this information it is possible to evaluate equation (C12) in a simple analytical fashion.

If one groups the integrand of equation (C12) as  $\tau(\alpha)$  and  $\alpha^{m+1}d\alpha$ , a partial integration yields

$$I_m = \frac{2}{\pi} \left\{ \frac{1}{m+1} [\tau(1) + (-1)^m \tau(-1)] - \frac{1}{m+1} \int_{-1}^1 \tau'(\alpha) \alpha^{m+1} d\alpha \right\} \quad (\text{E2})$$

Similarly, if one groups the integrand of the integral expression in equation (E2) as  $\tau'(\alpha)$  and  $\alpha^{m+1}d\alpha$ , a partial integration yields

$$I_m = \frac{2}{\pi} \left\{ \frac{1}{m+1} [\tau(1) + (-1)^m \tau(-1)] - \frac{1}{(m+1)(m+2)} [\tau'(1) + (-1)^{m+1} \tau'(-1) - P_m] \right\} \quad (\text{E3})$$

where

$$P_m = \int_{-1}^1 \tau''(\alpha) \alpha^{m+2} d\alpha \quad (\text{E4})$$

As a result of the parabolic-arc approximations of  $\tau(\alpha)$ ,  $\tau''(\alpha)$  is constant over each segment of arc as indicated by equation (E1). Hence, with the aid of equation (E1), equation (E4) can be written

$$P_m \approx \sum_{i=1}^{I-1} \tau''(\alpha_i) \int_{\alpha_i}^{\alpha_{i+1}} \alpha^{m+2} d\alpha$$

which, after integration, becomes

$$P_m \approx \frac{1}{m+3} \sum_{i=1}^{I-1} \tau''(\alpha_i) \left( \alpha_{i+1}^{m+3} - \alpha_i^{m+3} \right) \quad (\text{E5})$$

## REFERENCES

1. Jones, Robert T.: Theory of Wing-Body Drag at Supersonic Speeds. NACA Rep. 1284, 1956.
2. Holdaway, George H., and Mersman, William A.: Application of Tchebichef Form of Harmonic Analysis to the Calculation of Zero-Lift Wave Drag of Wing-Body-Tail Combinations. NACA RM A55J23, 1956.
3. Holdaway, George H.: Comparison of Theoretical and Experimental Zero-Lift Drag-Rise Characteristics of Wing-Body-Tail Combinations Near the Speed of Sound. NACA RM A53H17, 1953.
4. Levy, Lionel L., Jr., and Yoshikawa, Kenneth K.: A Numerical Method for Calculating the Wave Drag of a Configuration From the Second Derivative of the Area Distribution of a Series of Equivalent Bodies of Revolution. NASA MEMO 1-16-59A, 1959.
5. Baldwin, Barrett S., and Dickey, Robert R.: Application of Wing-Body Theory to Drag Reduction at Low Supersonic Speeds. NACA RM A54J19, 1955.
6. Sears, William R.: On Projectile of Minimum Wave Drag. Quart. Appl. Math., vol. 4, no. 4, Jan. 1947, pp. 361-366.
7. Beane, Beverly: The Characteristics of Supersonic Wings Having Biconvex Sections. Jour. Aero. Sci., vol. 18, no. 1, Jan. 1951, pp. 7-20.
8. Jarmalow, K., and Vandrey, F.: An Exact Method for the Rapid Calculation of the Area Distributions of Wings of Trapezoidal Geometry Based on a New Interpretation of the Area Rule. Eng. Rep. No. 7689, Glenn L. Martin Co., Aug. 24, 1955.



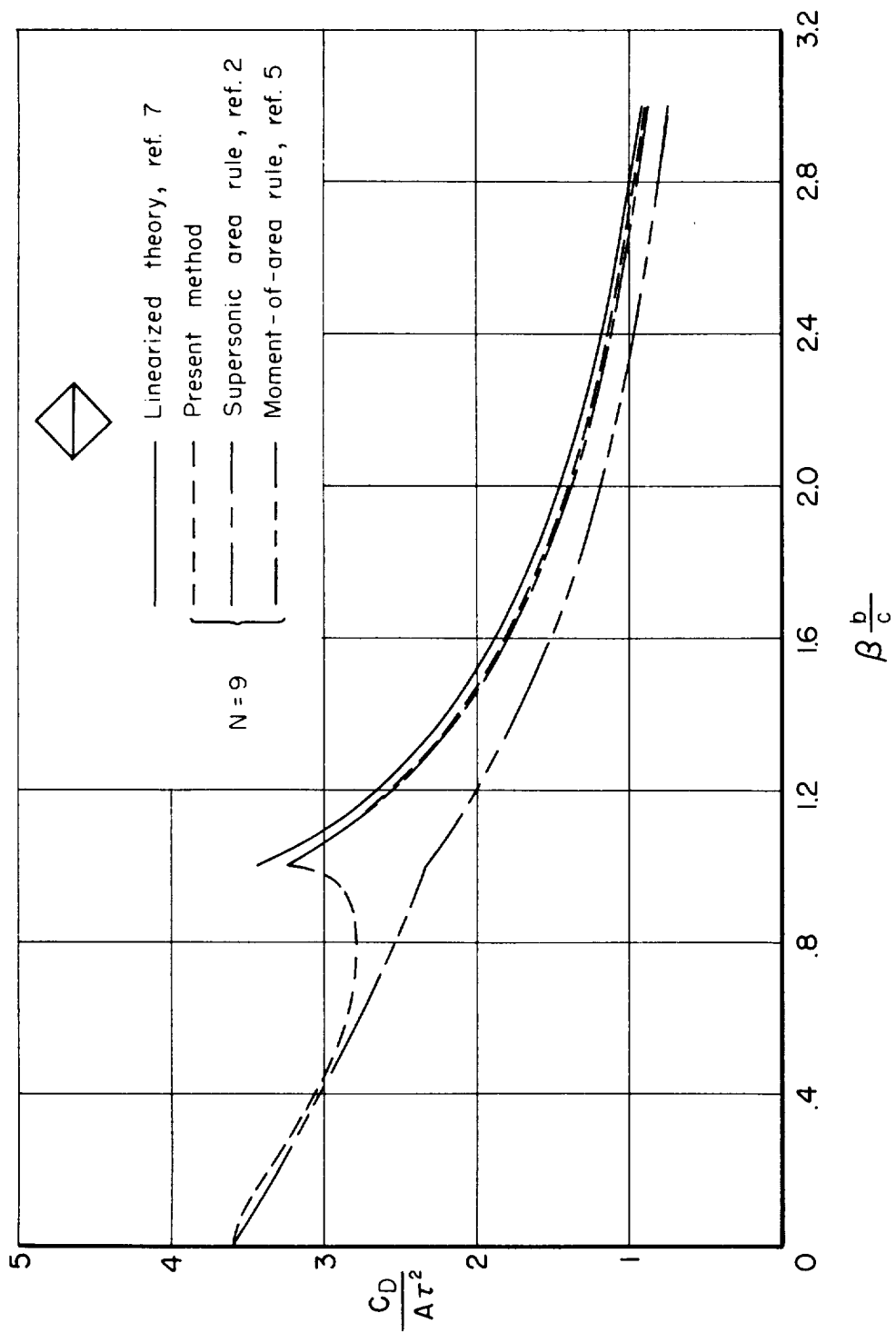
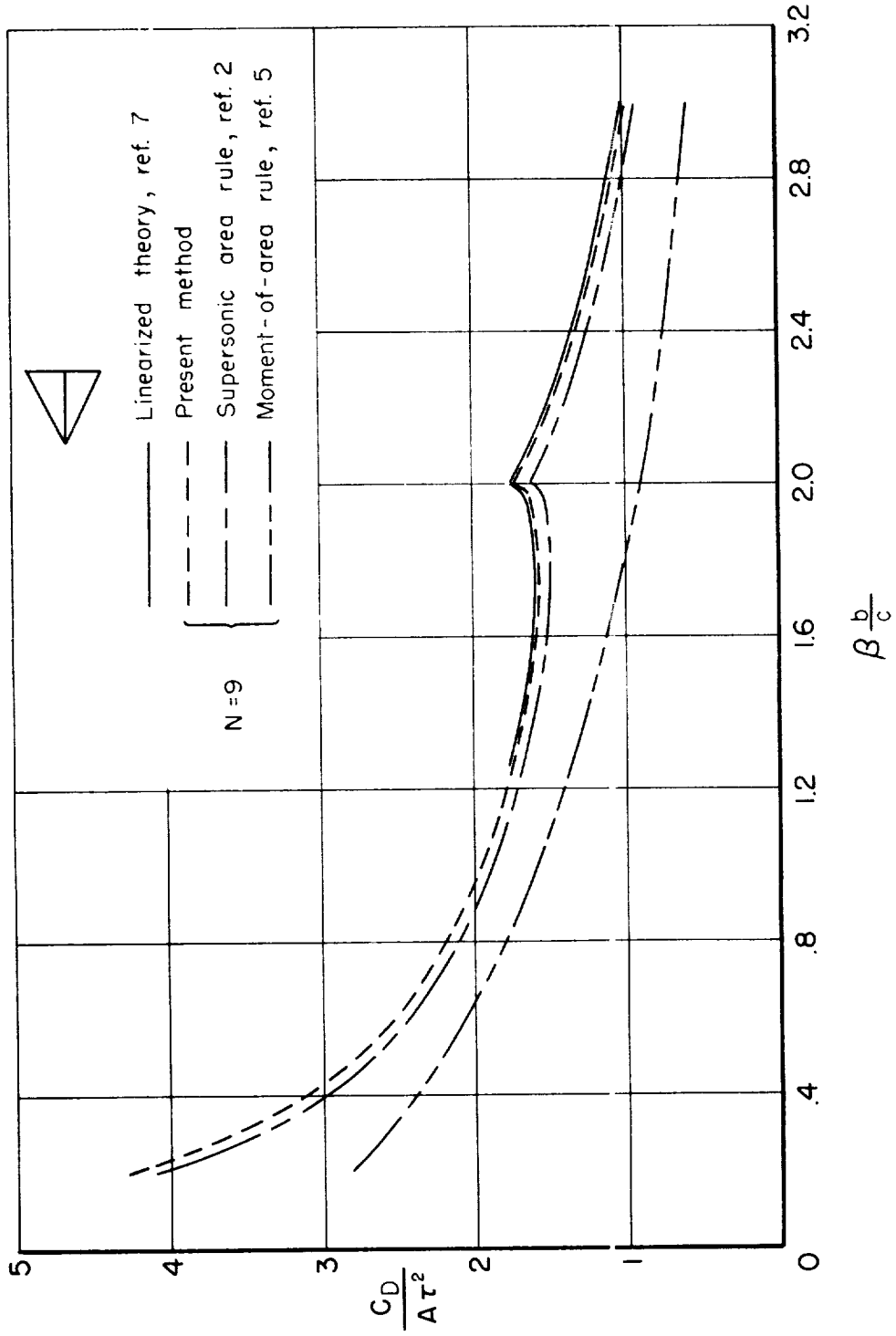
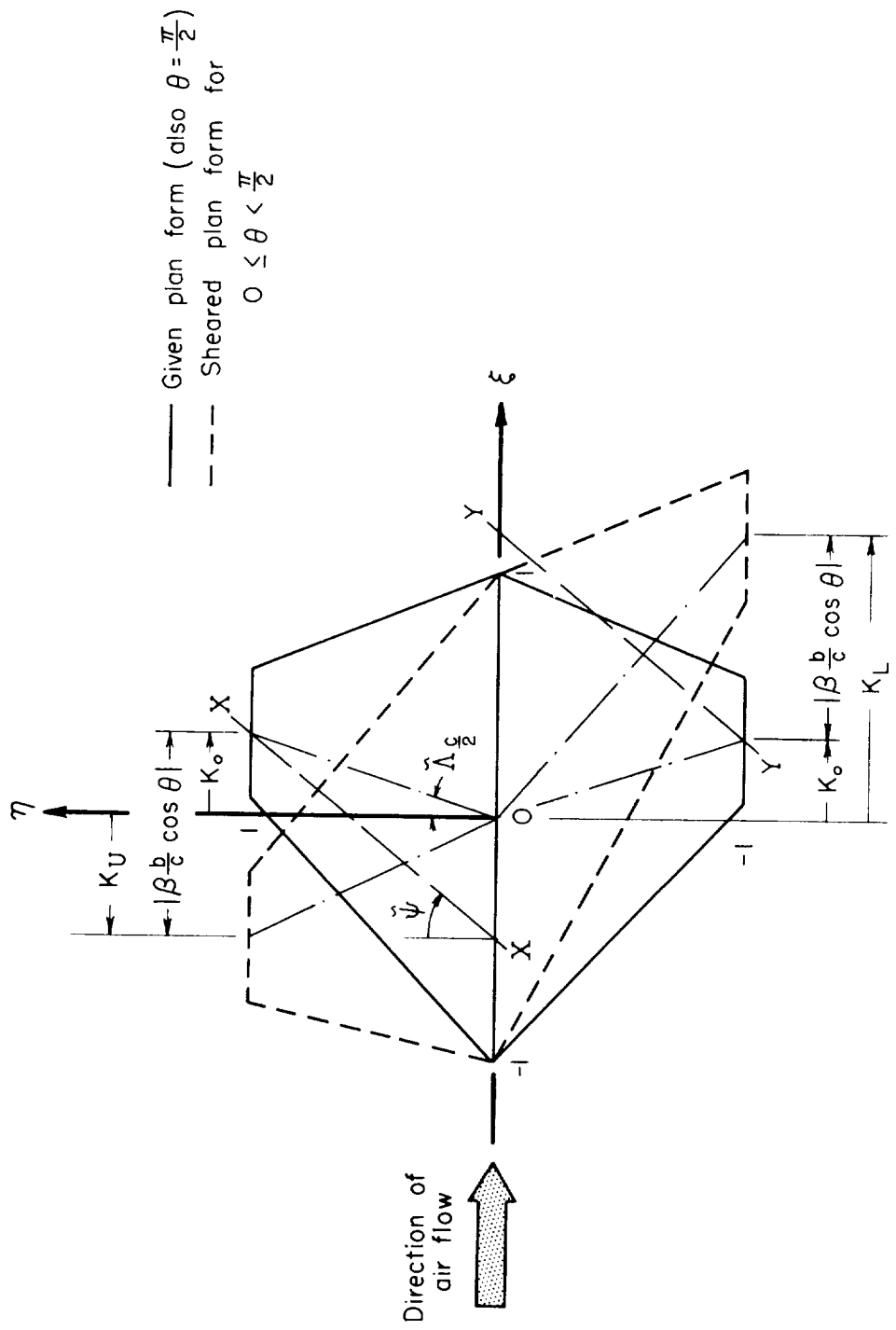


Figure 1.- Reduced zero-lift wave-drag coefficients for two plan forms with biconvex airfoil section of constant thickness ratio.



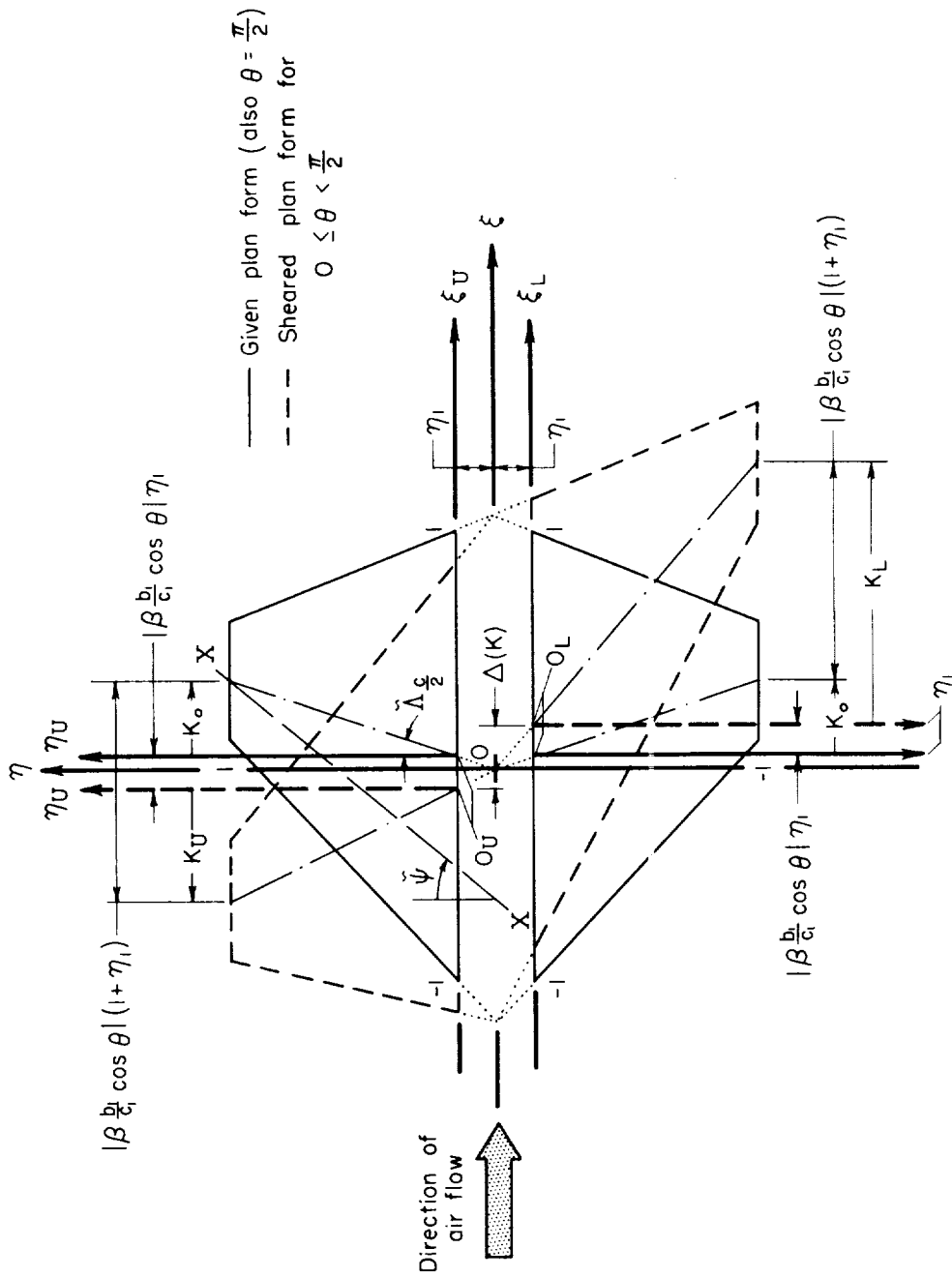
(b) Triangular plan form,  $K_0 = 1$

Figure 1.- Concluded.



(a) Complete wing

Figure 2.- Sketch, in dimensionless coordinates, showing a wing plan form and a typical sheared plan form.



(b) Exposed wing panels of a wing - body combination

Figure 2.- Concluded.

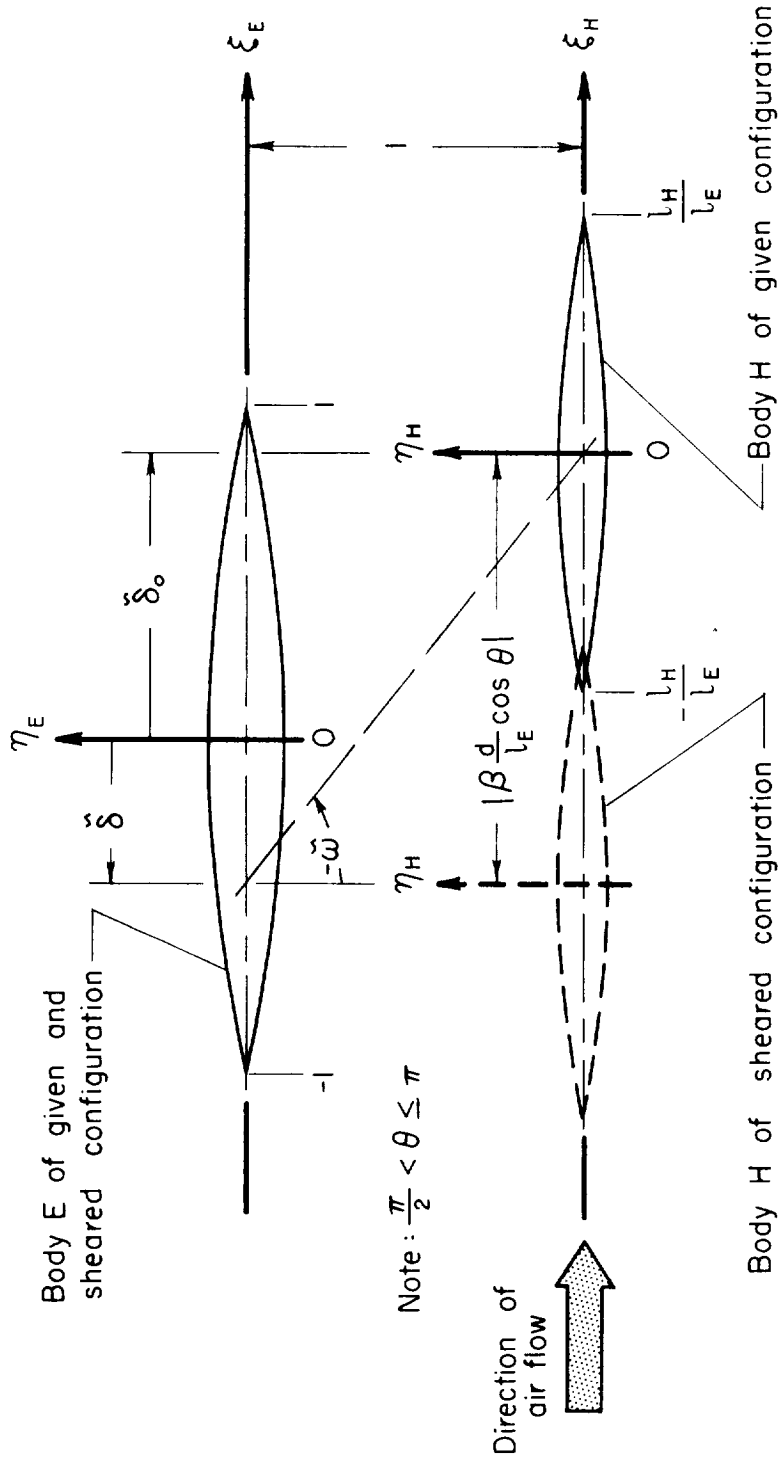


Figure 3.- Sketch, in dimensionless coordinates, showing a pair of bodies of revolution and a typical sheared configuration.

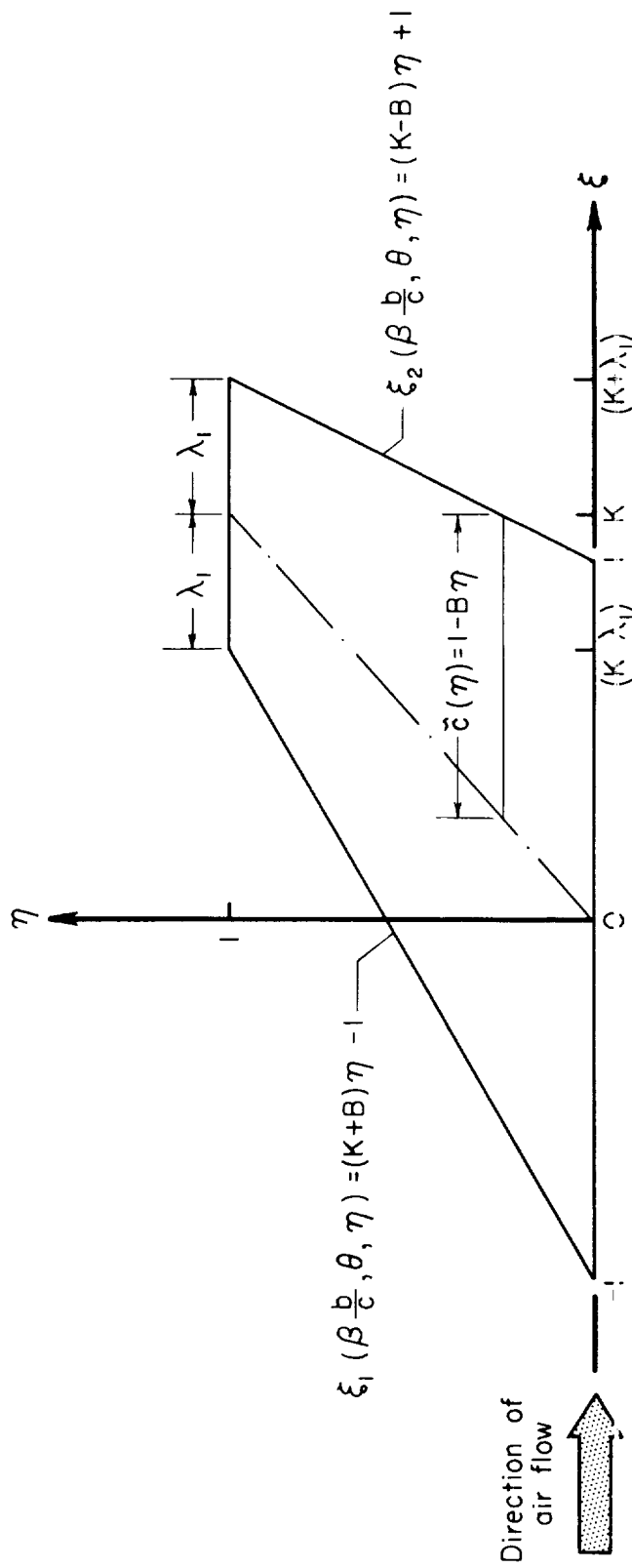


Figure 4.- Sketch, in dimensionless coordinates, showing a typical sheared exposed wing panel.

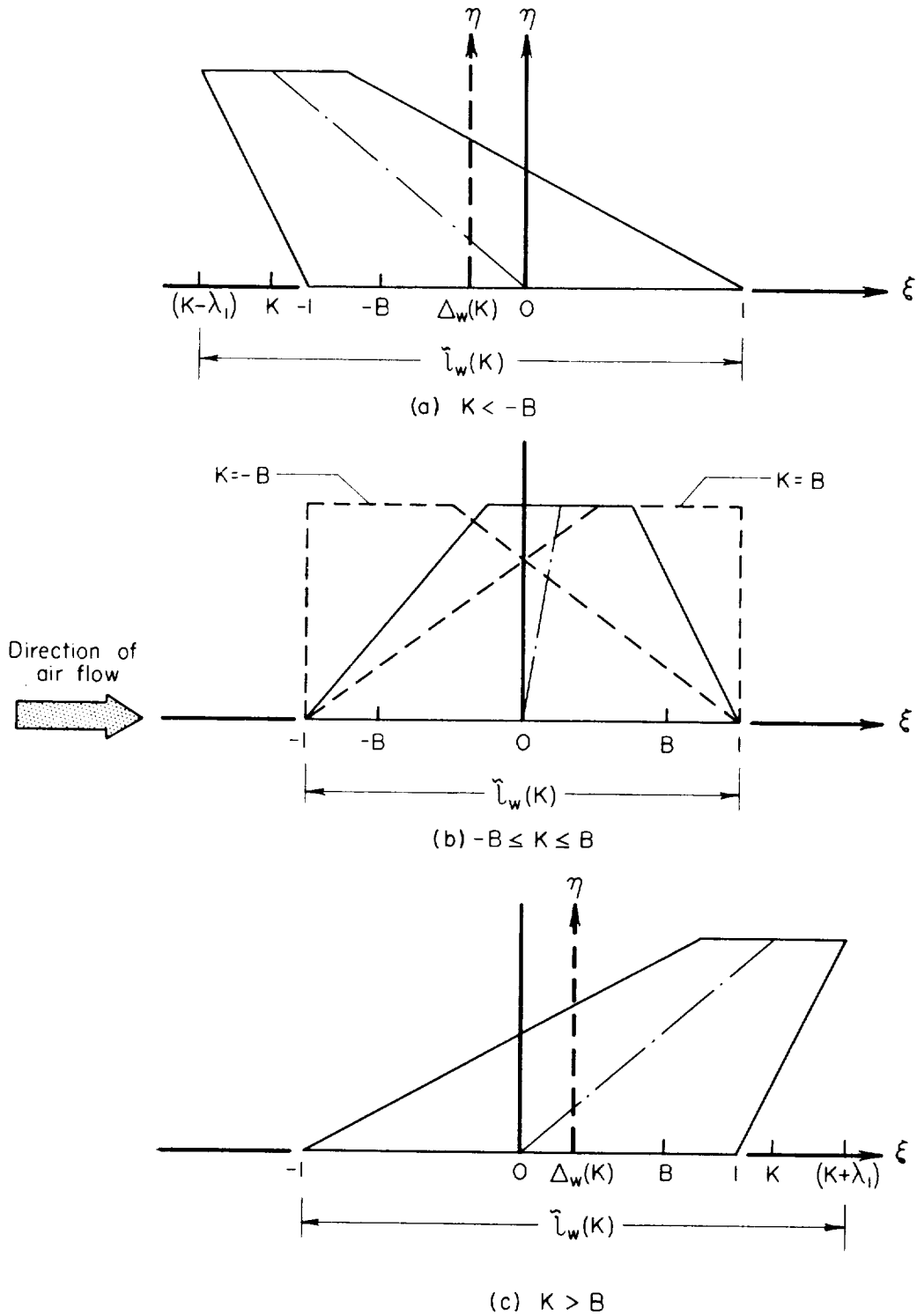
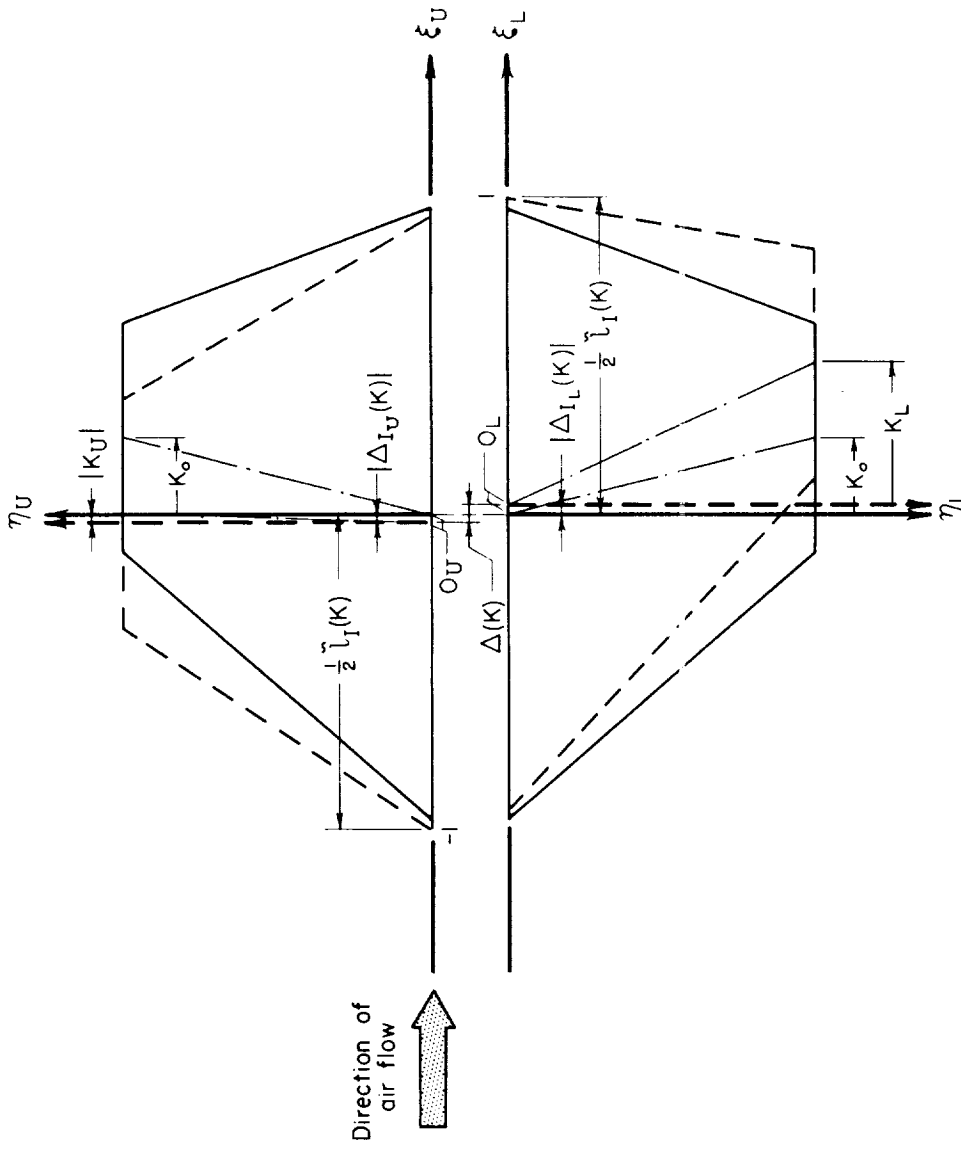
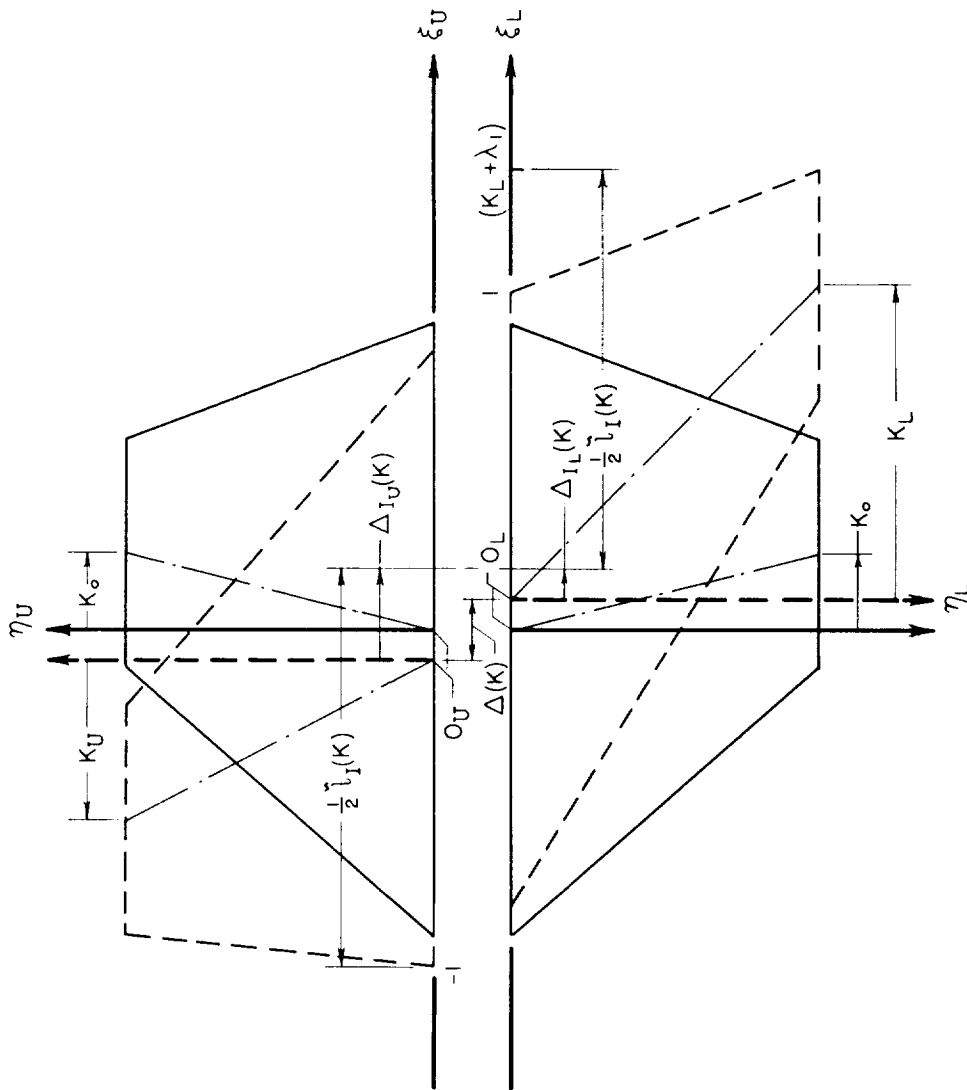


Figure 5.- Sketch, in dimensionless coordinates, showing lengths and moment transfer distances for sheared wing panels.



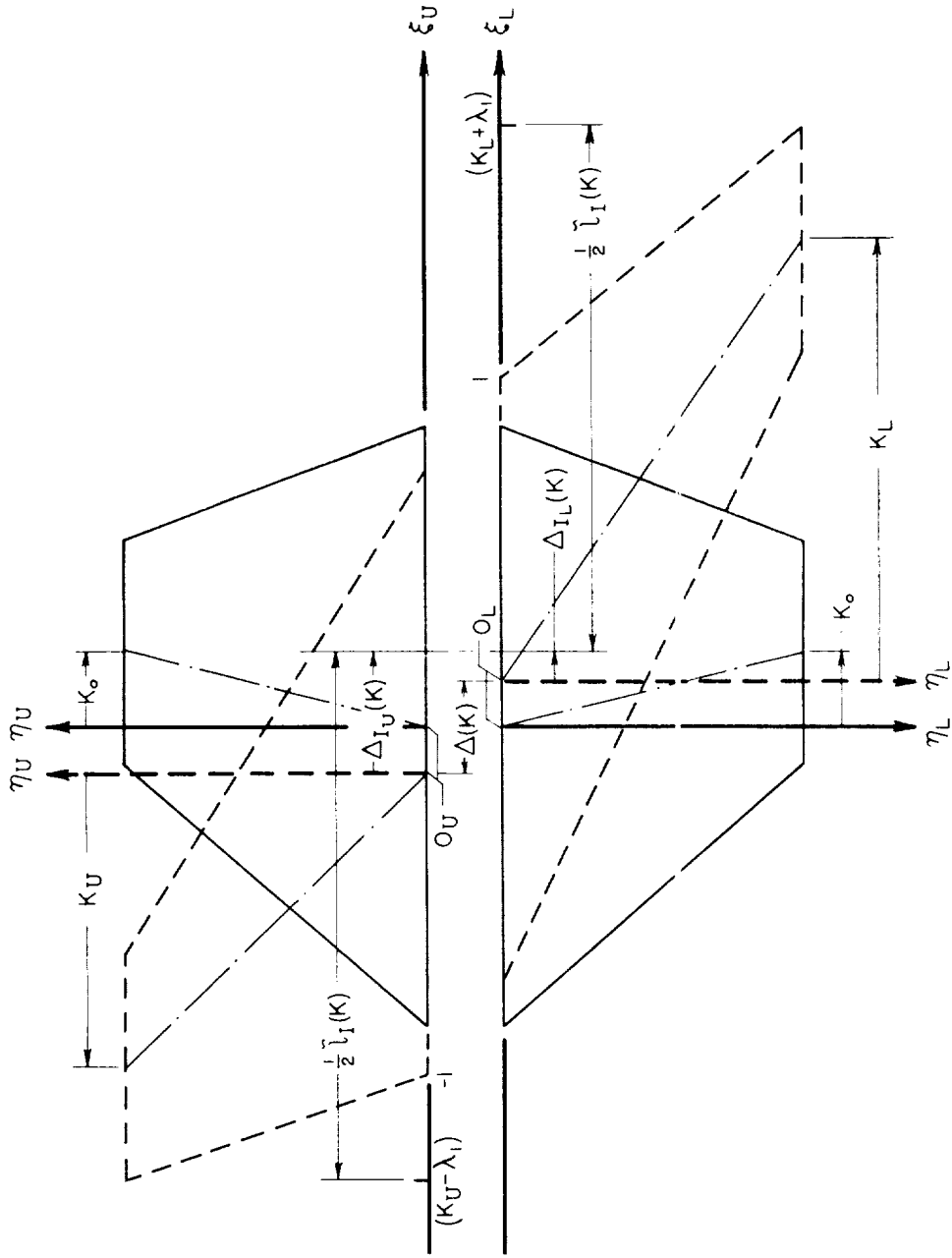
(a)  $0 \leq K_0 \leq B$ ,  $K_0 \leq K_L \leq B$

Figure 6.- Sketch, in dimensionless coordinates, showing lengths and moment transfer distances for sheared exposed plan forms.



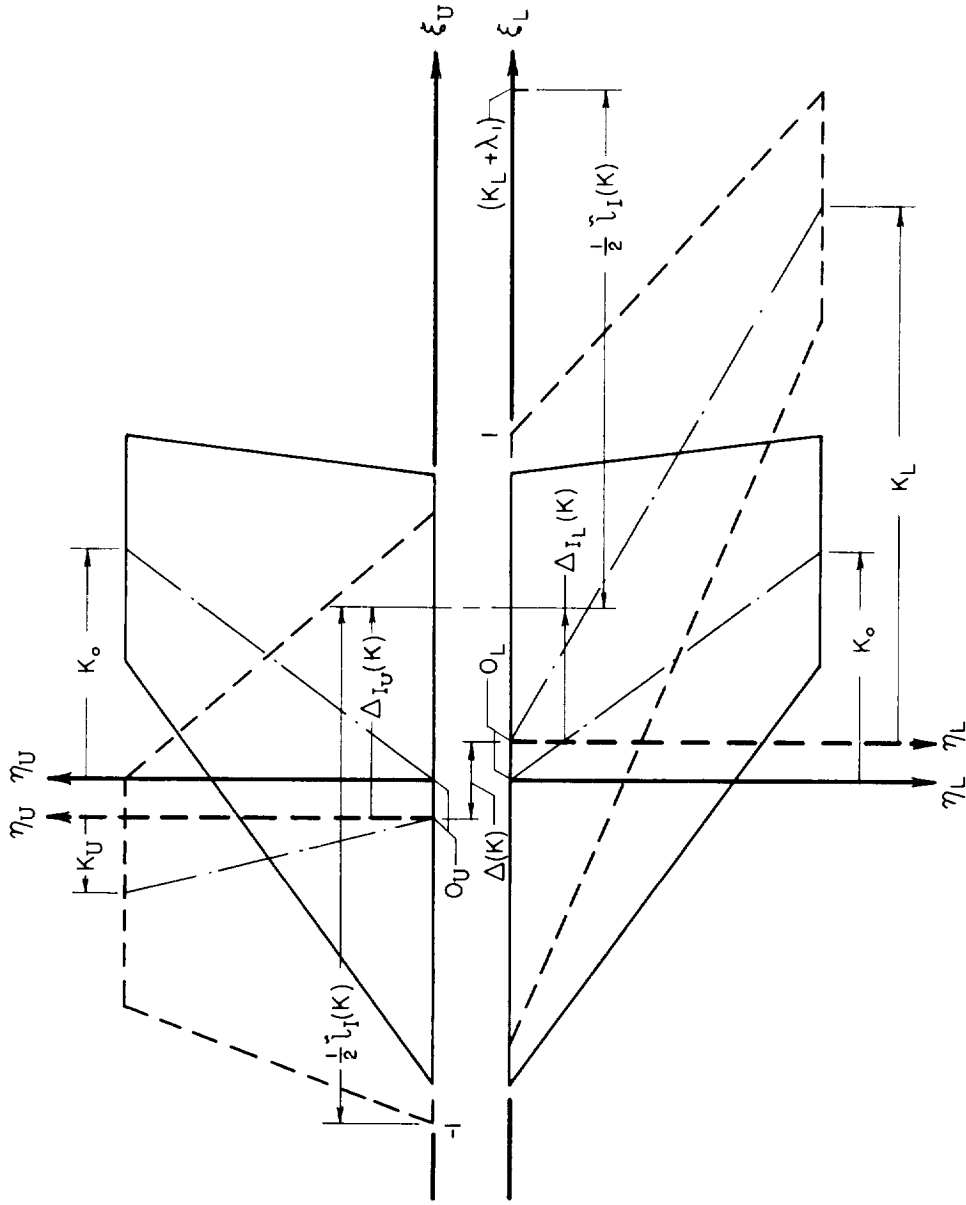
(b)  $0 \leq K_o \leq B$ ,  $B \leq K_L \leq (B + 2K_o)$

Figure 6.- Continued.



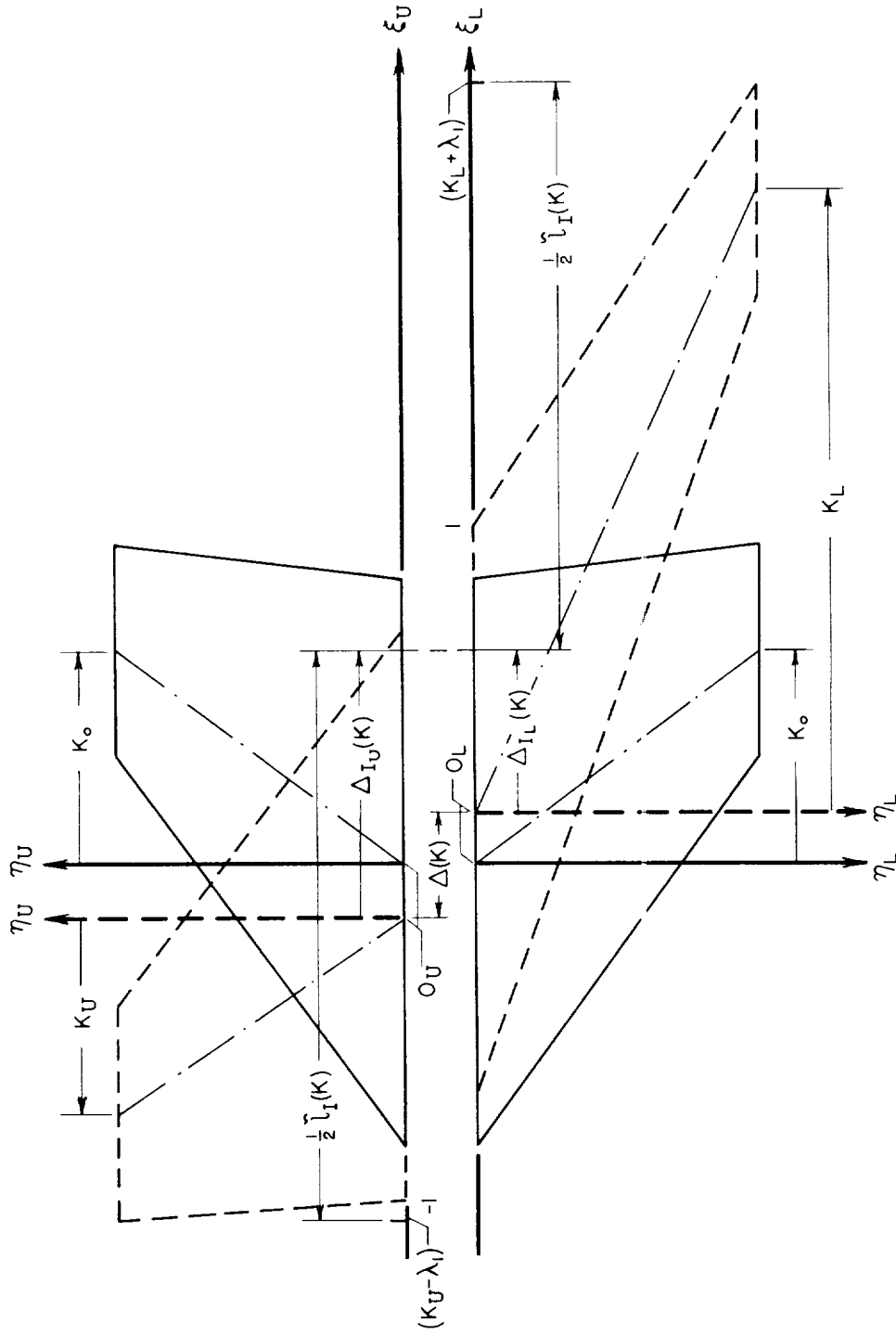
(c)  $0 \leq K_0 \leq B$ ,  $K_L > (B + 2K_0)$

Figure 6.- Continued.



(d)  $K_o > B$ ,  $K_o \leq K_L \leq (B + 2K_o)$

Figure 6.- Continued.



(e)  $K_o > B$ ,  $K_L > (B + 2K_o)$

Figure 6.- Concluded.

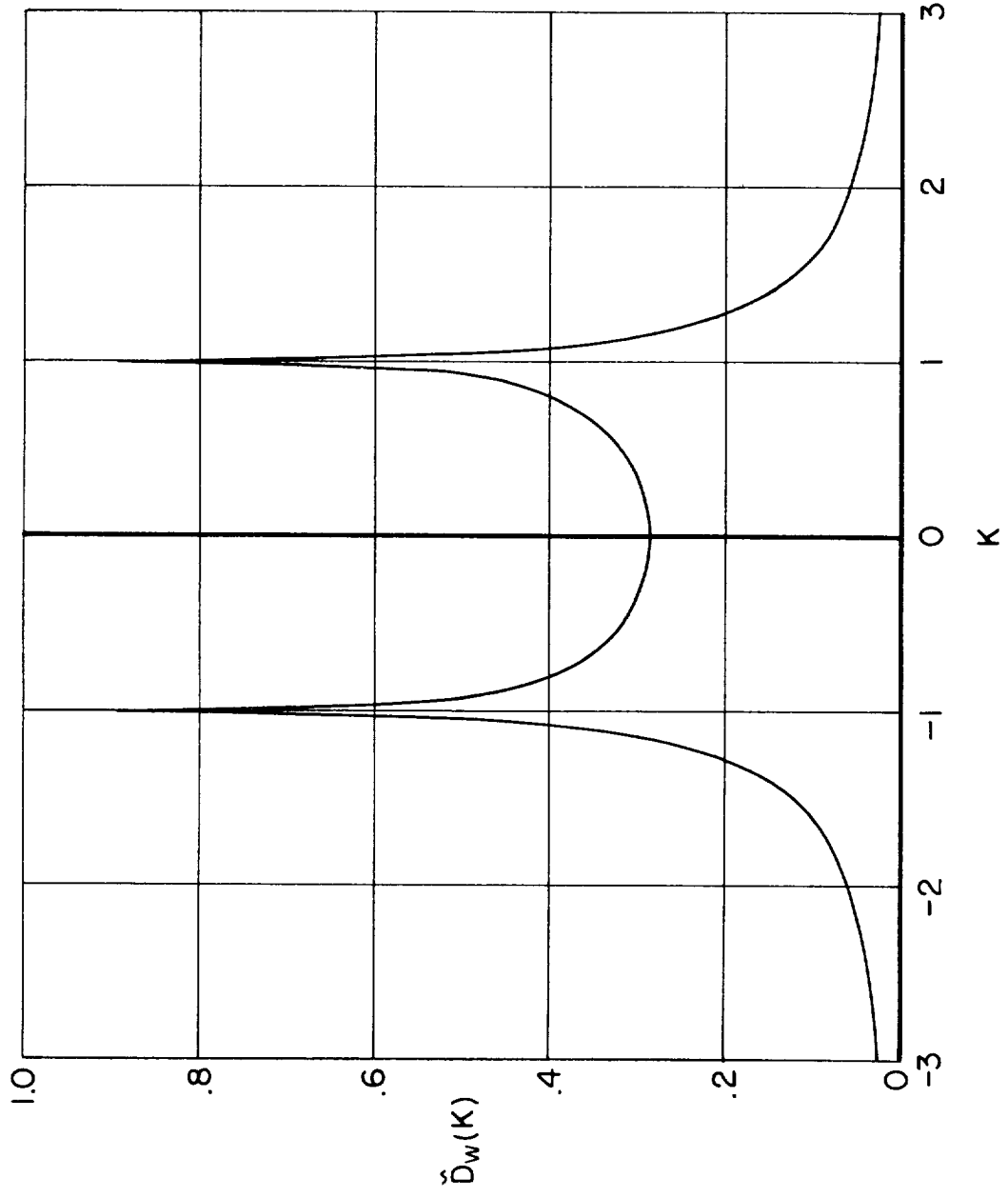


Figure 7.- Variation of dimensionless zero-lift wave drag with  $K$  for the sheared wing panels alone of appendix D.

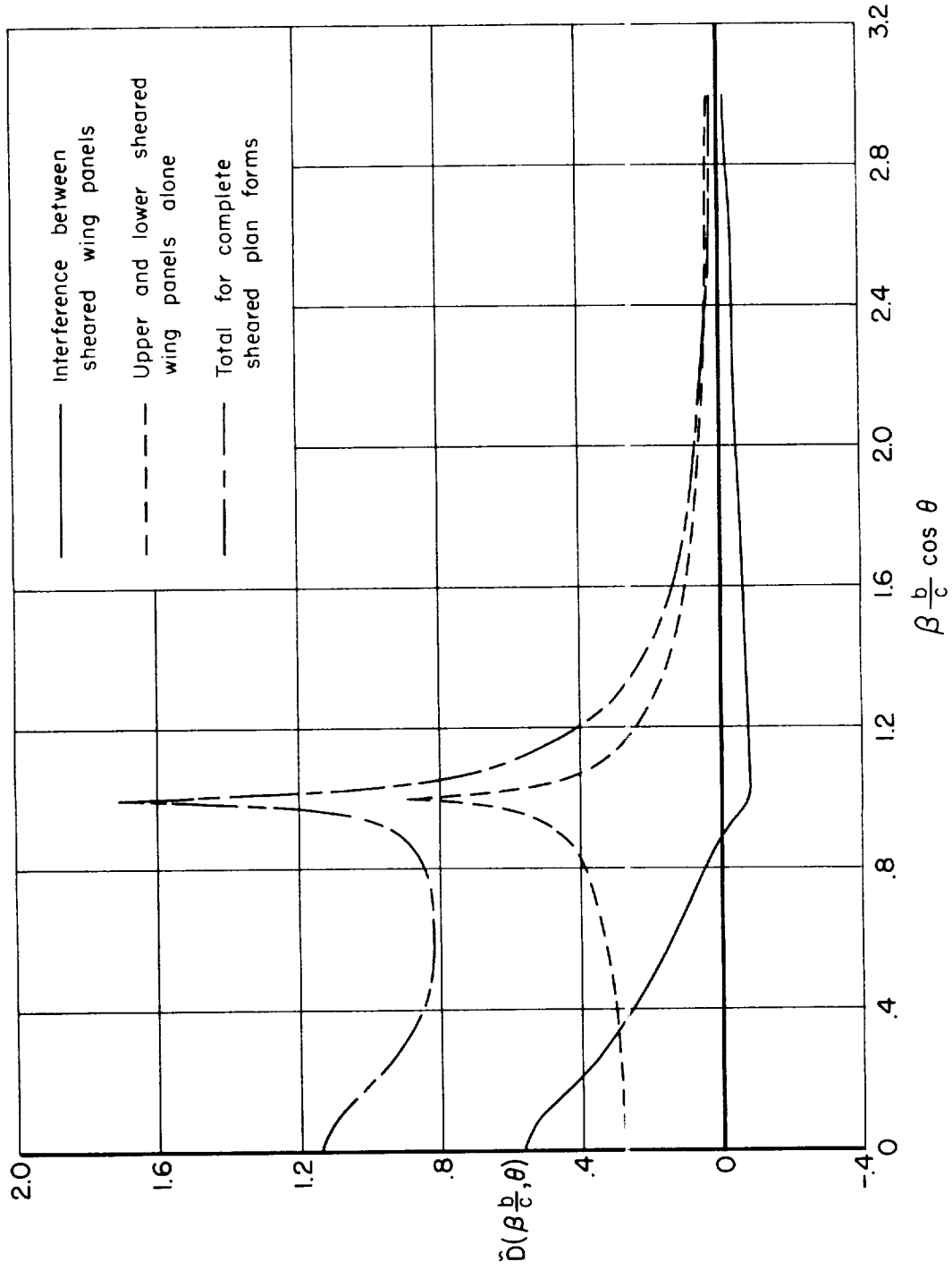


Figure 8.- Variation of dimensionless zero-lift wave drag with  $\beta b/c \cos \theta$  for the sheared components of the wings of appendix D.

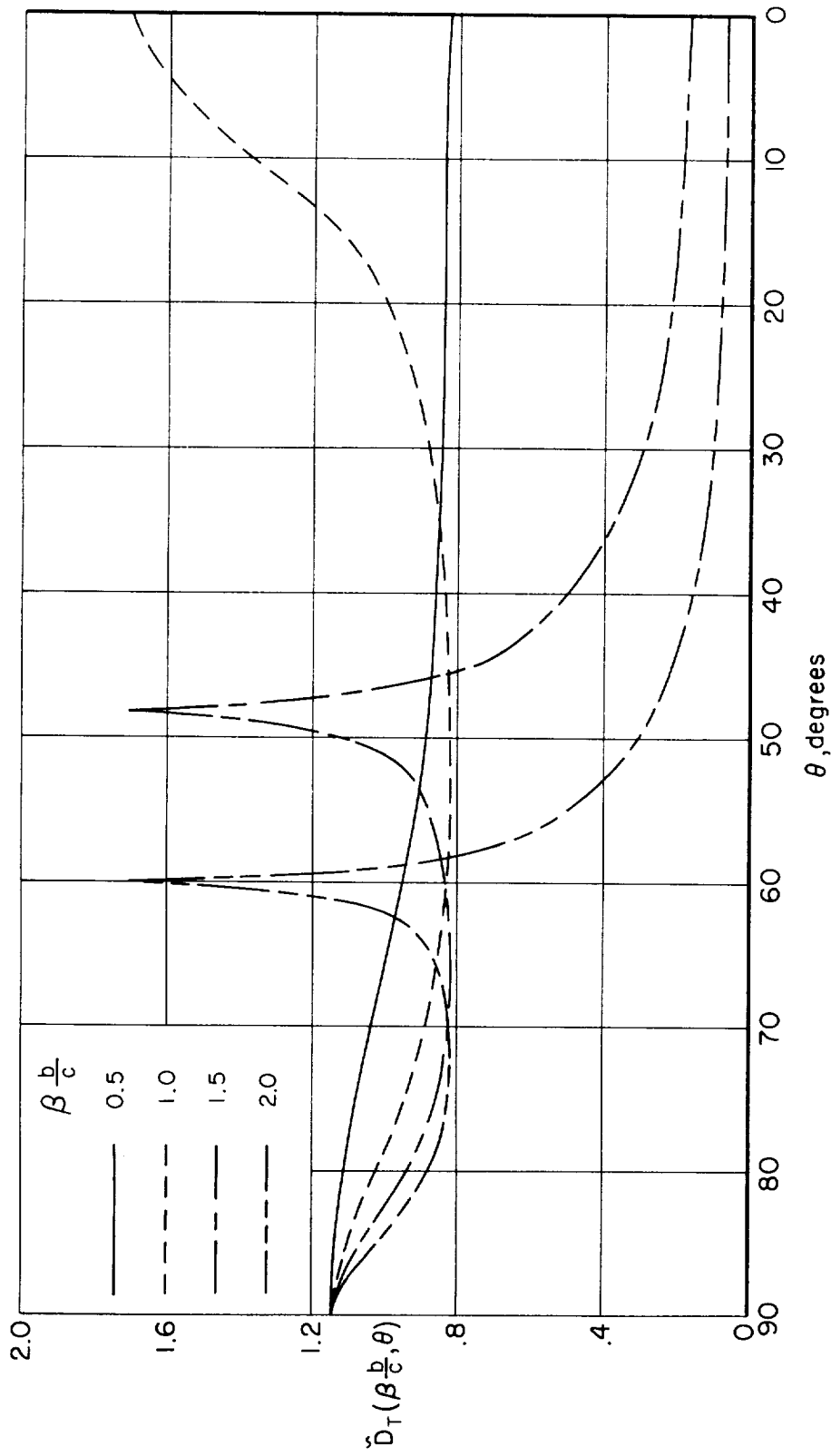


Figure 9.- Variation of the dimensionless total zero-lift wave drag with  $\theta$  for the sheared complete wings of appendix D.

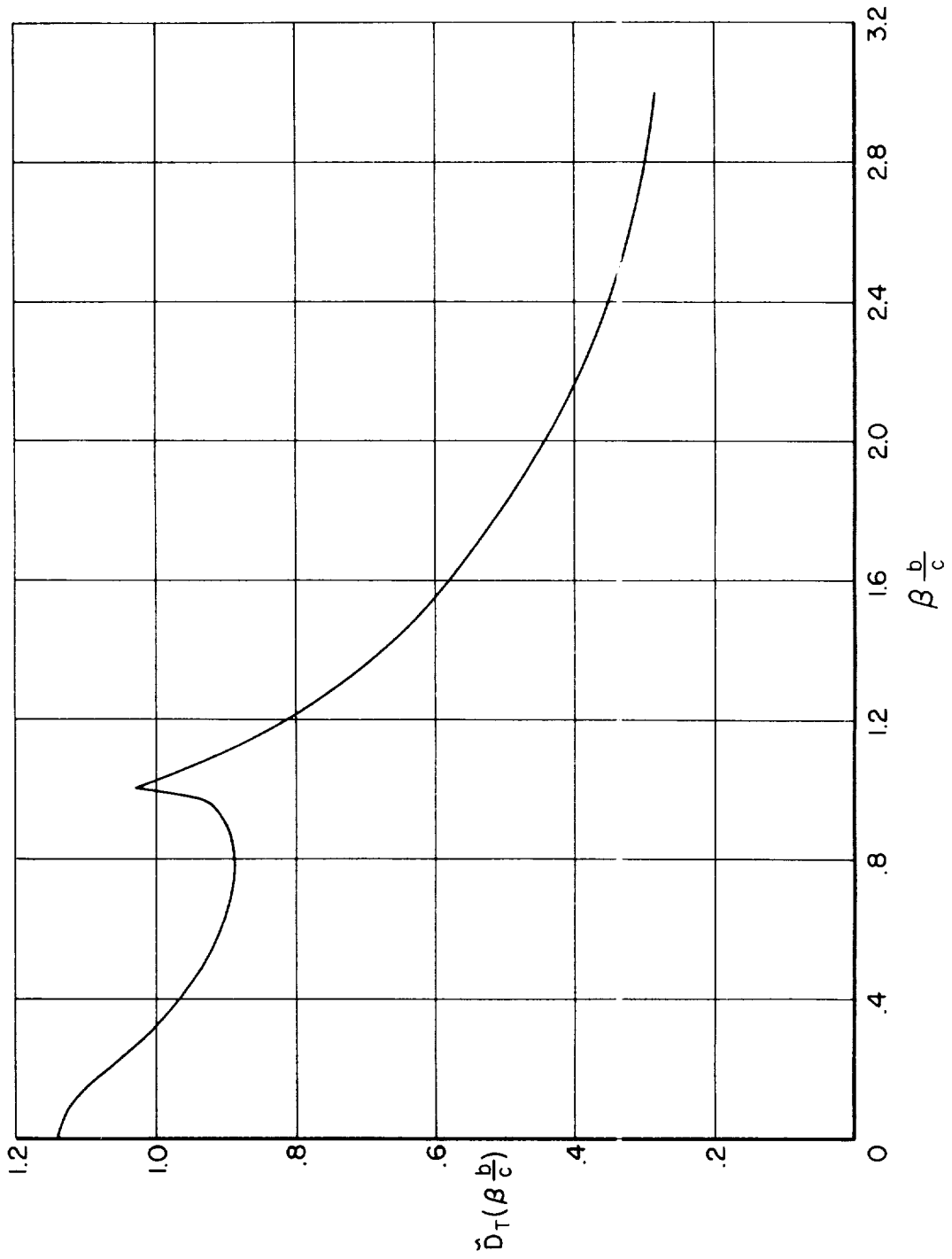


Figure 10.1.- Dimensionless total zero-lift wave drag for the complete wings of appendix D.